

72-1027 TN-68 AMENDMENT 1
TABLE OF CONTENTS

SECTION	PAGE
Appendix 3B STRUCTURAL ANALYSIS OF THE TN-68 BASKET	
3B.1	Introduction..... 3B.1-1
3B.1.1	Geometry..... 3B.1-1
3B.1.2	Weight..... 3B.1-2
3B.1.3	Temperature 3B.1-2
3B.2	Basket Finite Element Model Development (For Side Impact Analysis)..... 3B.2-1
3B.3	Basket Under Normal Condition Loads..... 3B.3-1
3B.3.1	Description 3B.3-1
3B.3.2	Basket Analysis Under 1G Side Load..... 3B.3-1
3B.3.3	Basket Analysis Under Vertical Load..... 3B.3-2
3B.3.4	Basket Thermal Expansion Analysis 3B.3-4
3B.3.5	Design Criteria 3B.3-6
3B.3.6	Evaluation 3B.3-7
3B.4	Basket Under Accident Condition Loads - Stress Analysis..... 3B.4-1
3B.4.1	Basket Analysis Under 60 g Bottom End Drop 3B.4-1
3B.4.2	Basket Analysis Under Tipover Side Impact..... 3B.4-2
3B.4.3	Design Criteria For Impact Accident..... 3B.4-2
3B.4.4	Evaluation 3B.4-3
3B.5	Basket Under Accident Condition Loads-Buckling Analysis..... 3B.5-1
3B.5.1	Analysis of Basket To Determine the Buckling Loads..... 3B.5-1
3B.5.2	Analysis Results 3B.5-3
3B.5.3	Evaluation 3B.5-5
3B.5.4	Analysis of the Aluminum Rails to Determine the Buckling Loads..... 3B.5-5
3B.5.5	Evaluation 3B.5-8
3B.6	Summary of Basket Structural Analysis 3B.6-1
3B.6.1	Stresses Due To Normal Condition Service 3B.6-1
3B.6.2	Stresses Due To Accident Condition 3B.6-2
3B.7	References 3B.7-1

72-1027 TN-68 AMENDMENT 1
TABLE OF CONTENTS

List of Tables

3B.3-1	Summary of Basket Stress Analysis - Normal Condition (1G Side Load)
3B.3-2	Linearized Stress Intensities of Aluminum Rail - Normal Condition (0° Side Load)
3B.3-3	Linearized Stress Intensities of Aluminum Rail - Normal Condition (30° Side Load)
3B.3-4	Linearized Stress Intensities of Aluminum Rail - Normal Condition (45° Side Load)
3B.4-1	Summary of Basket Stress Analysis - Accident Condition (Side Drop)
3B.4-2	Linearized Stress Intensities of Aluminum Rail - Accident Condition (0° Side Drop)
3B.4-3	Linearized Stress Intensities of Aluminum Rail - Accident Condition (30° Side Drop)
3B.4-4	Linearized Stress Intensities of Aluminum Rail - Accident Condition (45° Side Drop)

List of Figures

3B.1-1	Representative Basket Wall Panel
3B.2-1	Axial View of Basket
3B.2-2	Geometry for ANSYS Model
3B.2-3	Finite Element Model and Element Types
3B.2-4	Basket Finite Element Model - Stainless Steel Boxes
3B.2-5	Basket Finite Element Model - Stainless Steel Plates
3B.2-6	Basket Finite Element Model - Aluminum Rails
3B.3-1	Loading and Boundary Conditions - 0° Drop
3B.3-2	Loading and Boundary Conditions - 30° Drop
3B.3-3	Loading and Boundary Conditions - 45° Drop
3B.3-4	Membrane Stress Intensity (SS Plate) - 0 Degree Drop
3B.3-5	Membrane + Bending Stress Intensity (SS Plate) - 0 Degree Drop
3B.3-6	Membrane Stress Intensity (SS Box) - 0 Degree Drop
3B.3-7	Membrane + Bending Stress Intensity (SS Box) - 0 Degree Drop
3B.3-8	Membrane Stress Intensity (SS Plate)-30 Degree Drop
3B.3-9	Membrane + Bending Stress Intensity (SS Plate) - 30 Degree Drop
3B.3-10	Membrane Stress Intensity (SS Box) - 30 Degree Drop
3B.3-11	Membrane + Bending Stress Intensity (SS Box) - 30 Degree Drop
3B.3-12	Membrane Stress Intensity (SS Plate)- 45 Degree Drop
3B.3-13	Membrane + Bending Stress Intensity (SS Plate) - 45 Degree Drop
3B.3-14	Membrane Stress Intensity (SS Box) - 45 Degree Drop
3B.3-15	Nodal Stress Intensity (SS Plate) - 45 Degree Drop
3B.3-16	Nodal Stress Intensity (Aluminum Rails) - 0 Degree Drop
3B.3-17	Nodal Stress Intensity (Aluminum Rails) - 30 Degree Drop
3B.3-18	Membrane + Bending Stress Intensity (Aluminum Rails) - 45 Degree Drop
3B.3-19	Basket Stress Due to 3G Vertical Load
3B.3-20	Stress Report Location (Big Rail)
3B.3-21	Stress Report Location (Small Rail)
3B.3-22	Extraction of Partial Basket Model (Fusion Welds)
3B.3-23	Basket Partial Model (Fusion Welds)
3B.3-24	Basket Full Model (Fusion Welds)
3B.3-25	Locations of Basket Support Plates
3B.5-1	Drop Orientation
3B.5-2	Finite Element Model Simulation
3B.5-3	Finite Element Model Geometry
3B.5-4	Finite Element Model Plot
3B.5-5	Loading Conditions
3B.5-6	Boundary Conditions
3B.5-7	0° Drop Buckling Analysis - ANSYS Computer Plot
3B.5-8	10° Drop Buckling Analysis - ANSYS Computer Plot
3B.5-9	20° Drop Buckling Analysis - ANSYS Computer Plot
3B.5-10	30° Drop Buckling Analysis - ANSYS Computer Plot
3B.5-11	45° Drop Buckling Analysis - ANSYS Computer Plot

APPENDIX 3B

STRUCTURAL ANALYSIS OF THE TN-68 BASKET

3B.1 Introduction

This appendix presents the structural analysis of the TN-68 fuel support basket. The basket is a welded assembly of stainless steel boxes and designed to accommodate 68 fuel assemblies. The fuel compartment stainless steel box sections are attached together locally by fusion welds to 304 stainless steel plates sandwiched between the stainless steel walls of adjacent box sections. The basket contains 68 compartments for proper spacing and support of the fuel assemblies.

The basket structure is open at each end and therefore, longitudinal fuel assembly loads are directly on the cask body and not on the fuel basket structure. The fuel assemblies are laterally supported in the stainless steel structural boxes, and the basket is laterally supported by the rails and the inner shell of the cask.

The deformations and stresses induced in the basket structure due to the applied lateral loads are determined using the ANSYS computer program⁽¹⁾. The most severe loading for which the basket is evaluated is the hypothetical tipover accident as described in Section 3A.2.3.2. A 60 g vertical loading on the basket is also evaluated to represent a hypothetical end drop accident. Also a 3 g loading is applied to the basket in the vertical directions and 1 g loading is applied to the lateral direction as a bounding load to represent Level A (normal) Conditions. The inertial loads of the fuel assemblies are applied as equivalent densities on the stainless steel boxes. Quasistatic stress analyses are performed with applied loads in equilibrium with the reactions at the periphery of the basket. The calculated stresses in the basket structure are compared with the stress limits to demonstrate that the established design criteria are met.

3B.1.1 Geometry

The details of the TN-68 basket are shown on TN Drawing Nos. 972-70-4, and -5. As described above, the basket structure consists of an assembly of stainless steel boxes or cells joined by fusion welds and separated by stainless steel and poison plates. The stainless box, stainless steel plate and poison plate between fuel compartments is effectively a sandwich panel. The panel consists of one 0.3125 in thick 304 stainless steel plate and one 0.3125 in thick poison plate sandwiched between two 0.1875 in thick 304 stainless boxes. The 304 stainless steel members are the primary structural components. The poison plates provide the heat conduction path from the fuel assemblies to the cask cavity wall, and also provide criticality control.

A representative basket wall panel between fuel compartments is shown in Figure 3B.1-1. The panel plates are welded together at discrete locations (1 fusion weld every 12.17 inches) along their length. The adjacent fuel compartment stainless steel walls are fusion welded to both adjacent box sections. This method of construction forms a very strong honeycomb-like structure of boxes. The open dimension of each fuel compartment cell or box is 6.0 in x 6.0 in which provides a minimum of 1/8 in clearance around the fuel assemblies. The pitch of the cells is approximately 6.69 in. The overall basket length including spacer, (164 in + 13.25 in) 177.25

in, is less than the cask cavity length to allow for loading the fuel assemblies, thermal expansion and tolerance stackup.

Structural rails oriented parallel to the axis of the cask are attached to the periphery of the basket to establish and maintain basket orientation, to prevent twisting of the basket assembly, and to support the edges of those plates adjacent to the rails, which would otherwise be free to slide tangentially around the cask cavity wall under lateral inertial loadings.

3B.1.2 Weight

A value of 705 lb is assumed for the weight of each fuel assembly including fuel channels. Under lateral inertial loading each assembly is assumed to be uniformly supported across the width and along the length of the basket wall. The inertia of the basket structure (weight of the basket x g load) is also included in the analysis.

3B.1.3 Temperature

Thermal analyses are performed to obtain the temperature distributions in the basket for various conditions. These analyses are presented in Chapter 4. The effects of axial and radial thermal expansion of the basket are evaluated in Section 3B.3.4.

3B.2 Basket Finite Element Model Development (For Side Impact Analysis)

The basket model is an extremely large and complex ANSYS model. Because of the number of plates in the basket and the size of the basket, certain modeling approximations are necessary. The basket structure construction is repetitive symmetry (1 fusion weld every 12.17 inches along the length). It is practical to model only a single transverse slice (12.17 inches length) using a three-dimensional finite element model. The elements used in the model to represent the plates are Shell 63 quadrilateral shell elements and the rails are modeled by Solid 45 3D structural solid elements. For conservatism, the poison plates are not assumed to carry the structural load (except through the thickness support) and are not included in the model, but their weight (inertial load) is included in the stress calculation.

The fuel compartment corners and basket periphery are carefully modeled to define each plate connection. The connections between stainless steel boxes, stainless boxes and poison plates, stainless steel boxes and aluminum rails are made by node couplings. The nodes at the locations of fusion welds are coupled in all degrees of freedom (the fusion welds are rigidly connected the stainless steel boxes and stainless steel plates together at these nodes). The nodes of various plates are coupled together in the out of plane direction so that they will bend in unison under surface pressure or other lateral loading and to simulate the through thickness support provided by the poison plates. Figures 3B.2-1 and 2 show the typical basket panel ANSYS finite element model simulation. The component assembly model computer plot is shown on Figure 3B.2-3 and the individual component computer plots are shown on Figures 3B.2-4 to 3B.2-6.

3B.3 Basket Under Normal Condition Loads

3B.3.1 Description

The poison plates in the TN-68 basket are heat conductors and provide the necessary criticality control. The 304 stainless steel members are the primary structural components.

The poison plate strength is neglected (except for through thickness load transfer capability) under primary loading where the poison plate can share the load with the 304 stainless steel. This analysis approach produces conservatively high calculated values of primary stresses in the stainless steel components. The primary stress analysis of the basket under the bounding loads for Level A is described below.

3B.3.2 Basket Analysis Under 1 g Side Load

Finite Element Model

The ANSYS finite element model described in Section 3B.2 is used to perform the structural analysis of the basket.

Loading

The basket is analyzed for 0°, 30°, and 45° lateral loads to bound the possible maximum stress cases. The lateral load orientation angles are defined in Figures 3B.3-1, 3B.3-2, and 3B.3-3.

All analysis is based on 1g acceleration. The loading due to poison plates and fuel assembly weight are applied as equivalent densities. The poison plate weight is distributed on all four sides of stainless steel boxes, and the fuel assembly weights are distributed on the top panel of the SST-AL-SST sandwich for the 0° lateral load orientation and proportionally distributed on the top & side panels for the 30° and 45° lateral load orientations.

Boundary Conditions

The boundary condition at each point of contact between the basket and cask body cavity depends on the direction of the applied inertial load. As the basket is forced in a particular lateral direction, it separates from the cask wall on one side and reacts against the wall on the other side. At the locations where the basket loses contact with the wall, no restraint or support is provided in the model. For vertical inertial loading on a horizontal cask and basket, contact is lost between the basket and cask wall at the top half of the structure. The load distributions and boundary conditions are shown on Figures 3B.3-1 through 3B.3-3.

Material Properties

The material properties of the 304 stainless steel plates are taken from ASME⁽²⁾ Code, Section II, Part D. The material properties of the aluminum alloy (6061-T6) are also taken from the ASME

Code. These properties are listed with specific reference in Chapter 3. Chapter 4 shows the temperature distribution at various locations of the basket and rails. The maximum calculated temperatures for the various sections of the basket and rails are also summarized in Chapter 4. Based on this thermal analysis, the maximum basket temperature is 595°F and the maximum rail temperature is 382°F. The structural analysis of the basket and rails conservatively assumes a uniform temperature of 600°F for basket and 400°F for the rails.

Analysis and Stress Results

Analyses using the basket system model are performed for the 0°, 30°, and 45° lateral load orientations relative to the basket plates as indicated in Figures 3B.3-1 through 3B.3-3. In all cases, the analyses for the individual loads are performed using the linear elastic method so that ratios can be used to obtain stress results for specified loads. Detailed stress, displacements, and forces in the finite element model are available in ANSYS output files. These results were postprocessed. The nodal stress intensities and deformed geometry for 0°, 30°, and 45° load cases are plotted in Figures 3B.3-4 through 3B.3-18. The stress intensities shown in figures are calculated based on an average fuel assembly weight of 705 lb (the entire fuel assembly weight is conservatively assumed to act on 144" basket length only) and are summarized in Tables 3B.3-1 to 3B.3-4. These maximum stresses are evaluated below to verify that the design criteria are met.

3B.3.3 Basket Analysis Under Vertical Load

Under vertical loads, the fuel assemblies and basket are forced against the bottom of the cask. It is important to note that, for any vertical or near vertical loading, the fuel assemblies react directly against the bottom of the cask cavity and not through the basket structure as in lateral loading.

3 g Vertical Load - 304 Stainless Steel

The analysis of the basket subjected to the 3 g bounding vertical load (bounds all Level A, Normal Conditions) for the panels with poison plate is shown in Figure 3B.3-19. A full length of compartment wall (164 in long) with a span length of 6.375 in is evaluated for compressive loading. A maximum compressive force of (3×163) 489 lb occurs at the bottom of the wall. Stresses are conservatively calculated by assuming all of the load is taken by the 304 stainless steel. Therefore

$$\sigma = \text{Total Compressive Load/Cross Section of 304SS} = 489 \text{ lb}/2.39 \text{ in}^2 = 205 \text{ psi} \approx 0.21 \text{ ksi}$$

There are cutouts in 4 locations at the bottom of the basket for lifting. In addition there are drain slots (1.0" wide \times 1.0" high) at the bottom of the basket. For these locations, an analysis of the vertical g loadings has been evaluated for each box section.

$$\text{Total weight of one box section (164" long)} = 163 \text{ lb} \times 4 = 652 \text{ lb}$$

$$\text{Total area} = (2.39 \text{ in}^2 \times 4) \times (17.3/25.5) = 6.49 \text{ in}^2$$

$$\sigma = \text{Total Compressive Load/Cross Section of 304SS} = (652 \times 3) \text{ lb}/6.49 \text{ in}^2 = 301 \text{ psi} \approx 0.3 \text{ ksi}$$

Based on the above results it is concluded that the stresses in the stainless steel panel due to the 3 g vertical load are insignificant (much less than the allowable stress of 14.76 ksi, Section 3B.3.5).

Stainless Steel Fusion Weld

Under the vertical load, each fusion weld is designed to support a panel including one 0.3125" thick \times 10.4" high \times 6.1875" span poison plate and one 0.3125" thick \times 1.75" high \times 6.1875" span stainless steel, therefore, the total weight of this panel is:

$$W = (0.3125" \times 10.4" \times 6.1875") \times 0.1 \text{ lb/in}^3 + (0.3125" \times 1.75" \times 6.1875") \times 0.29 \text{ lb/in}^3 = 3 \text{ lb}$$

$$\text{Under 3 g vertical load, the shear stress, } \tau = 3W/A = 3(3)/[\pi(0.5)^2/4] = 46 \text{ psi} \approx 0.05 \text{ ksi}$$

This shear is much less than the allowable shear stress of 2.95 ksi (Section 3B.3.5).

3 g Vertical Load - Aluminum Rails

Under vertical load, each rail is designed to support its own weight. The weight and areas of the rail are:

	Area (in ²)	Weight (164" long),lb
Small Rail (Figure 3B.3-21)	8.78	145
Large Rail (Figure 3B.3-20)	16.34	270

Therefore, the maximum compressive stress under 3 g vertical load is:

$$\sigma_1 = 145 \times 3/8.78 = 49.54 \text{ psi} \approx 0.05 \text{ ksi}$$

$$\sigma_2 = 270 \times 3/16.34 = 49.57 \text{ psi} \approx 0.05 \text{ ksi}$$

These compressive stresses are much less than the allowable stress of 4.5 ksi (Section 3B.3.5)

3B.3.4 Basket Thermal Expansion Analysis

The thermal analyses of the basket under various conditions are described in Chapter 4. The temperatures from those thermal analyses are used to evaluate the effects of axial and radial thermal expansion in the basket components.

Thermal Expansion between Fuel Assembly / Basket / Cask

In order to prevent thermal stress, adequate clearance is provided between the basket outer diameter and cask cavity inside diameter, basket axial length and cask cavity length, and fuel assembly axial length and cask cavity length for free thermal expansion. Expansion is checked for three cases with the 30 kW design basis heat load:

- 1) Long term normal condition, 100°F ambient, 0.10 inch hot gap at perimeter of basket (Section 4.3.5, Table 4.3-1 “Average temp at hottest cross section”)
- 2) Vacuum drying at 30 hours, with radial gap between basket and cask wall (Section 4.5.1, Table 4.5-2, “Avg temperature at hottest cross section, 0.1 inch hot gap”)
- 3) Vacuum drying at 30 hours, no radial gap between basket and cask wall (Section 4.5.1, Table 4.5-2 “Avg temperature at hottest cross section, 0.0 hot gap”)

Case 2 is the bounding condition for internal basket and fuel temperatures, and therefore it is the bounding case for axial expansion of the fuel and the basket relative to the cask, pairs B and C in the table below. Case 3 pair A demonstrates that if the basket comes into contact with the cavity wall, as assumed in Section 4.5.1, the resulting drop in the basket temperature will result in an equilibrium condition with a small radial gap between the basket and shell.

Summary of gaps between adjacent components of the TN-68 Storage Cask

Pair	Differential Expansion Between Components	Material	Long Term 100°F Ambient Case 1		Vacuum w/radial gap Case 2		Vacuum no radial gap Case 3	
			Avg Temp (°F)	Min Gap (in)	Avg Temp (°F)	Min Gap (in)	Avg Temp (°F)	Min Gap (in)
A	Basket OD	SA-240 Type 304	479	0.011	--	Note 1	433	0.02
		Aluminum Rail	366		--		258	
	Cask ID	SA-203 Gr. E	316		--		252	
B	Fuel Assembly length	Zircaloy/ 304 S.S.	622	0.362 Note 2	752	0.158 Note 2	--	Note 3
	Cask Cavity length	SA-203 Gr. E	316		223		--	
C	Basket length	SA-240 Type 304	479	0.317	534	0.101	--	Note 3
		Aluminum Poison plate	366		400		--	
	Cask Cavity length	SA-203 Gr. E	316		223		--	

Notes:

1. The gap is not calculated because this case assumes by definition that a radial gap exists, as the basis for calculating the maximum temperatures of basket components and fuel.
2. Includes consideration of 0.36 inch of axial free space taken up by damaged fuel end caps
3. This is not the bounding case for axial expansion, because contact of the basket perimeter with the cavity wall results in reduced basket and fuel temperatures.

Thermal Expansion between the Basket Stainless Steel Support Plates and Aluminum Poison Plates

The TN-68 basket design includes gaps in both the transverse and axial directions to accommodate differential thermal expansion between the basket stainless steel plate and the neutron absorber plate. The following evaluation demonstrates that these gaps are adequate for the bounding normal condition for cask internal temperatures, vacuum drying with a radial gap between the basket and cask, case 2 above. All plates are assumed to be at the average temperature, 568°F, of the longest absorber plate calculated using a cross-section model with no axial heat transfer (Section 4.5.1).

Thermal Expansion Between Basket Stainless Steel and Poison Plates (Radial Direction)

There are four (4) different lengths of basket plates in the radial direction; the thermal expansion calculations are based on nominal plate length. The differential thermal expansions between

stainless steel and poison plates at these four different locations are:

$$\Delta_1 = 66.94 \times (14.136 - 9.8) \times 10^{-6} \times (568-70) = 0.145 \text{ inch}$$

$$\Delta_2 = 53.81 \times (14.136 - 9.8) \times 10^{-6} \times (568-70) = 0.116 \text{ inch}$$

$$\Delta_3 = 40.44 \times (14.136 - 9.8) \times 10^{-6} \times (568-70) = 0.087 \text{ inch}$$

$$\Delta_4 = 13.69 \times (14.136 - 9.8) \times 10^{-6} \times (568-70) = 0.03 \text{ inch}$$

Therefore, at these locations, minimum spaces of 0.15 in., 0.13 in., 0.1 in., and 0.05 in. are provided between stainless steel and poison plates (poison plate will be cut short) to allow free thermal expansion.

Thermal Expansion Between Basket Stainless Steel and Poison Plates (Axial Direction)

There are thirteen (13) poison plate sections (see Figure 3B.2-1) along the axial direction, the nominal height of the poison plate is 10.4", therefore, the maximum differential thermal expansion between the poison and stainless steel plates at 568°F is:

$$\Delta = 10.4 \times (14.136 - 9.8) \times 10^{-6} \times (568-70) = 0.022 \text{ inch}$$

Therefore, a minimum clearance of 0.023" is provided to permit free thermal expansion.

Based on the above calculations, adequate clearances have been provided for thermal expansion. Thus no thermal stress will be induced in the baskets.

Conclusion

Based on the above calculation, adequate clearances have been provided for thermal expansion. Thus no thermal stress will be induced in the basket.

3B.3.5 Design Criteria

The basis for the 304 stainless steel fuel compartment box section stress allowables is Section III, Subsection NG of the ASME⁽³⁾ Code. The primary membrane stress intensity and primary membrane plus bending stress intensities are limited to S_m (S_m is the Code allowable stress intensity) and $1.5 S_m$, respectively, at any location in the basket for Level A (Normal Service) load combinations. The average primary shear stress across a section is limited to $0.6 S_m$.

The ASME Code provides a basic $3 S_m$ limit on primary plus secondary stress intensity for Level A conditions. That limit is specified to prevent ratcheting of a structure under cyclic loading and to provide controlled linear strain cycling in the structure so that a valid fatigue analysis can be performed. The Code also provides guidance in the application of plastic analyses which can be performed to demonstrate shakedown (absence of ratcheting) and to determine stresses for

fatigue evaluation. Ratcheting and fatigue cannot occur in the basket since thermal cycling will not occur in this basket design. The numerical values of primary stress intensity limits are list in the following table.

TN-68 Basket Structural Design Criteria for Level A Conditions

Numerical Values of Primary Stress Intensity Limits			
	304 SS at 600°F (ksi)	SB 221, 6061-T6 Aluminum Rails at 400°F, (ksi)	ASME Reference
Membrane Stress Intensity $P_m (S_m)$	14.76 *	4.50	Subsection NG NG-3221.1
Membrane + Bending Stress Intensity $P_m + P_b (1.5 S_m)$	22.14*	6.75	Subsection NG NG-3221.2
Shear Stress at 600°F (Fusion Weld) $\tau (0.6 S_m)$	2.95**	-----	Subsection NG NG-3227.2 Table NG-3352-1

* The allowables were reduced ($\times 0.9$) to include the quality factor for full penetration based on progressive MT or PT examination (NG-3352)

** The allowables were reduced ($\times 0.3$) to include the quality factor for fusion weld based on visual examination (NG-3352)

3B.3.6 Evaluation

Stainless Boxes and Stainless Plates

Tables 3B.3-1 lists the stress intensities for the 1 G side load in the basket due to 0°, 30°, and 45° drop orientations. Note that these stresses have been calculated elastically (assuming structurally ineffective poison plates). The highest membrane stress intensity is 0.36 ksi. The highest membrane plus bending stress intensity is 0.63 ksi. These stresses are well below the allowable membrane stress intensity of 14.76 ksi and the allowable membrane plus bending stress intensity 22.14 ksi based on a basket temperature of 600°F.

Stainless Steel Fusion Welds

The ANSYS computer code is used to calculate the shear stresses at the fusion welds. Two drop orientations are analyzed. A partial finite element model for the 0° drop analysis was constructed with the following modifications using the finite element model described in Section 3B.2.

0° side impact

- Figure 3B.3-22 shows the full basket model and the section where the partial models will be extracted and modified for fusion weld shear stress calculations.
- Removed all aluminum rail elements (SOLID45). Also removed all the shell elements, except one center vertical row of elements as shown in Figure 3B. 3-23 for 0° side impact orientation. All the boundary conditions and couplings at the unused nodes were removed.
- Symmetry boundary conditions were applied at the cut surfaces.
- Removed the couplings at the fusion welds and replaced them with Elastic Pipe Element (PIPE16) of 0.5" outer dia. and 0.25 " thickness. The diameter of pipe elements for the 0° side impact model at the symmetry boundaries was reduced to 0.3536" (thickness = 0.1768) for 1/2 section area.
- All material properties, real constants and couplings of the reduced models are the same as described in Section 3B.3.2. The element and node numbers are, however, compressed in the partial models.

The maximum shear force in pipe element due to 1g load = 8.5 lb

Therefore, average shear stress = $8.5 / (\pi/4 \times 0.5^2) = 43 \text{ psi}$

45° Side Impact

A full model was considered better than a partial model for a 45 degree side drop, because it avoids complex symmetry boundary conditions at two cut sections needed for a partial model.

The ANSYS full finite element model and material properties were taken from Section 3B.3. The couplings at the fusion weld locations of the model are replaced with Elastic Pipe Element (PIPE16) of 0.5" outer diameter and 0.25" thickness. The finite element model and boundary conditions are shown in Figure 3B.3-24.

1g resultant load was applied using a factor of -0.707 in X-direction and 0.707 in Y-direction. The detailed resulting stresses and displacements are given in ANSYS file.

The maximum shear force in pipe element due to 1g load = 10.7 lb

Therefore, Avg. Shear Stress = $10.7 / (\pi/4 \times 0.5^2) = 55 \text{ psi}$

It is seen that the maximum average shear stress of 55 psi occurs in the fusion welds during a 45 degree-oriented side drop under 1g load.

The allowables at 600° F are:

Allowable = $0.3 \times 0.6 \times 16.4 = 2.95 \text{ ksi}$

Therefore, Normal Condition Allowable 'g' load = $2.95 / 0.055 = 54$

Aluminum Rails

The maximum nodal stress intensities of the aluminum rails due to 0°, 30°, and 45° drop orientations are plotted in Figures 3B.3-16 through 3B.3-18. However, the final results of interest for comparison to design criteria are membrane and bending stress intensities. The stress components are processed to obtain the averaged membrane stress across each cross section and the linearized membrane plus bending stress. The cross section for averaging and linearization is defined by a path consisting of two ends or surface points (model nodes). The stress components through the section are linearized by the ANSYS postprocessor and separated into constant membrane stresses, P_m , and bending stresses, P_b , which varies linearly between the end points. The values of the principal stresses are determined from the stress components and the membrane and membrane plus bending stress intensities are calculated from these principal stresses. The critical sections in Figures 3B.3-20 and -21 are selected because of high nodal stresses at these locations and also for a potential of high linearized membrane and membrane plus bending stress intensities. The small rail (item 30, drawing no. 972-70-5) is not selected for a detailed evaluation as this rail acts just like a shim and is not subjected to any bending or column action.

Table 3B.3-2 lists the linearized stress intensities at each of the critical cross sections as shown on Figures 3B.3-20 and 21 for the 0° side load. The maximum membrane stress intensity in the basket is 0.11 ksi at location 1 and the maximum membrane plus bending stress intensity is 0.15 ksi also at location 1. These stress values are much less than the allowables for general membrane stress intensity of 4.5 ksi and membrane plus bending stress intensity of 6.75 ksi.

Table 3B.3-3 lists the linearized stress intensities at each of the critical cross sections as shown on Figures 3B.3-20 and 21 for the 30° side load. The maximum membrane stress intensity in the basket is 0.08 ksi at location 1 and the maximum membrane plus bending stress intensity is 0.11 ksi also at location 1. These stress values are less than the allowables for general membrane stress intensity of 4.5 ksi and membrane plus bending stress intensity of 6.75 ksi.

Table 3B.3-4 lists the linearized stress intensities at each of the critical sections as shown on Figures 3B.3-20 and 21 for the 45° side load. The maximum membrane stress intensity in the basket is 0.06 ksi at location 1 and the maximum membrane plus bending stress intensity is 0.08 ksi also at location 1. These stress values are also less than the allowables for general membrane stress intensity of 4.5 ksi and membrane plus bending stress intensity of 6.75 ksi.

Based on the results of these analyses, it is concluded that:

1. The maximum stresses in the 304 stainless steel (fuel compartment) both in the stainless steel plates and stainless steel boxes of the basket, are well below the specified allowable stresses under normal service condition (1 g side load and 3g vertical load).

2. The maximum shear stress in the fusion welds is low under the 1 g side load and 3 g vertical load above.
3. The maximum membrane and membrane plus bending stress intensities of the aluminum rails are low.
4. The basket is structurally adequate and it will properly support and position the fuel assemblies under normal loading conditions.

3B.4 Basket Under Accident Condition Loads - Stress Analysis

3B.4.1 Basket Analysis Under 60 g Bottom End Drop

Appendix 3D presents the dynamic impact analysis of the TN-68 cask during a hypothetical end drop and tip over accidents. The maximum calculated impact g load for an 18 in vertical drop is 37 g. This section evaluates the basket stresses for a 60 g vertical load which is a conservative representation of the end drop. Appendix 3B.3.3 presents the analysis of the basket due to a 3 g vertical load neglecting the strength contribution from the poison plates (weight of poison plate is included in the calculation). It is conservatively assumed that all the load is taken by the 304 stainless steel. Therefore, the maximum compressive stress due to the 60 g end drop is:

$$\sigma_1 = \text{Total Comp. Load/Cross Section of 304SS} = (163 \times 60) \text{ lb}/2.39 \text{ in}^2 = 4,092 \text{ psi} \approx 4.1 \text{ ksi}$$

There are cutouts in 4 locations at the bottom of the basket for lifting. In addition there are drain slots (1" wide \times 1.0" high) at the bottom of the basket. For these locations, an analysis of the vertical g loadings has been performed for each box section.

$$\text{Total weight of one box section (164" long)} = 163 \text{ lb} \times 4 = 652 \text{ lb}$$

$$\text{Total area} = (2.39 \text{ in}^2 \times 4) \times (17.3/25.5) = 6.49 \text{ in}^2$$

$$\sigma_2 = \text{Total Comp. Load/Cross Section of 304SS} = (652 \times 60) \text{ lb}/6.49 \text{ in}^2 = 6,028 \text{ psi} \approx 6.03 \text{ ksi}$$

These stresses are less than the Level D membrane stress intensity limit for 304 stainless steel of 39.36 ksi (Section 3B.4.3).

Stainless Steel Fusion Weld

Under the vertical load, each fusion weld is designed to support a panel including one 0.3125" thick \times 10.4" high \times 6.1875" span poison plate and one 0.3125" thick \times 1.75" high \times 6.1875" span stainless steel, therefore, the total weight of this panel is:

$$W = (0.3125" \times 10.4" \times 6.1875") \times 0.1 \text{ lb/in}^3 + (0.3125" \times 1.75" \times 6.1875") \times 0.29 \text{ lb/in}^3 = 3 \text{ lb}$$

$$\text{Under 60 g end impact, the shear stress, } \tau = 60W/A = 60 (3)/[\pi (0.5)^2/4] = 917 \text{ psi} \approx 0.92 \text{ ksi}$$

This shear is much less than the allowable shear stress of 19.68 ksi (Section 3B.4.3).

60 g Vertical Load - Aluminum Rails

Under vertical load, each rail is designed to support its own weight. The weight and area of the rails are:

	Area (in ²)	Weight (164" long), lb
Small Rail (Figure 3B.3-21)	8.78	145
Big Rail (Figure 3B.3-20)	16.34	270

Therefore, the maximum compressive under 60 g end impact load is:

$$\begin{aligned}\sigma_1 &= 145 \times 60 / 8.78 = 990.9 \text{ psi} \approx 1.0 \text{ ksi} \\ \sigma_2 &= 270 \times 60 / 16.34 = 991.4 \text{ psi} \approx 1.0 \text{ ksi}\end{aligned}$$

These compressive stresses are much less than the membrane allowable stress of 10.8 ksi (Section 3B.4.3).

3B.4.2 Basket Analysis Under Tipover Side Impact

This section describes the analysis of the TN-68 basket in the unlikely event of cask tipover on a concrete pad. The design criteria established for the TN-68 basket for the hypothetical accident condition are described in Section 3B.4.3. These criteria were selected to ensure that the basket is structurally adequate under the tipover impact loads. The results from the analyses presented in this section are evaluated against the design criteria in Section 3B.4.3.

To determine the structural adequacy of the basket due to the cask tipover accident, the same drop orientations as described in Section 3B.3.2 are used to evaluate the basket stresses. Since those individual load cases are linear and elastic, their results can be ratioed and superimposed as required in order to perform the normal and hypothetical accident load combinations. Tables 3B.4-1 through 3B.4-4 list the maximum "membrane" & "membrane plus bending" stress intensities of the basket and rails due to 1g at 0°, 30°, and 45° side impacts. These stress intensities are compared with the Level D allowables to calculate the corresponding maximum allowable g loads.

3B.4.3 Design Criteria For Impact Accident

The stress criteria are taken from Section III, Appendix F of ASME⁽⁶⁾ Code. The hypothetical impact accidents are evaluated as short duration Level D conditions. For elastic analysis, the primary membrane stress is limited to the smaller of $2.4S_m$ or $0.7S_u$ and membrane plus bending stress intensities are limited to the smaller of $3.6S_m$ or S_u . The average primary shear stress

across a section is limited to the smaller of $0.42 S_u$ or $2 \times 0.6S_m$.

The fuel compartment walls, when subjected to compressive loadings, are also evaluated against ASME Code rules for component supports to ensure that buckling will not occur. The acceptance criteria (allowable buckling loads) are taken from ASME Code, Section III, Appendix F, paragraph F-1341.4, Plastic Instability Load. The allowable buckling load is equal to 70% of the calculated plastic instability load. The numerical values of Level D stress limits are listed in the following table.

TN-68 Basket Structural Design Criteria for Level D Conditions

Numerical Values of Primary Stress Intensity Limits			
	304 SS at 600°F (ksi)	SB 221, 6061-T6 Aluminum Rails at 400°F, (ksi)	ASME Reference
Membrane Stress Intensity P_m , (smaller of $2.4S_m$ or $0.7S_u$)	39.36	10.8	Appendix F F-1331.1a
Membrane + Bending Stress Intensity, $P_m + P_b$ (smaller of $3.6S_m$ or S_u)	59.04	16.0	Appendix F F-1331.1c
Shear Stress (Fusion Weld) τ , (smaller of $0.42 S_u$ or $2 \times 0.6S_m$)	19.68	-----	Appendix F F-1331.1d or NG-3225

3B.4.4 Evaluation

Based on the above analyses and results list in Tables 3B.4-1 through 3B.4-4, it is concluded that:

1. The maximum allowable G load for the stainless steel basket assembly is 94G. This G load is much higher than the calculated G load of 77 as described in Appendix D.
2. The maximum allowable G load for the aluminum rails is 98G.

3B.5 Basket Under Accident Condition Loads - Buckling analysis

3B.5.1 Analysis of Basket to Determine the Buckling Loads

Additional analyses are performed in this section to evaluate the outer basket plate stability when the lateral inertial loading is applied at various angles relative to the plates. Analyses are performed for 0, 10, 20, 30, and 45 degree drop angles (Figure 3B.5-1).

The basic structural element of the basket is considered to be a wall between fuel compartments which consists of 0.3125" thick stainless steel plate sandwiched between two 0.1875" thick stainless steel plates (the strength of poison plate is neglected from buckling load calculation, but its own weight is included). The overall dimensions of this outer basket wall are 6.1875" high and 12.17" wide (12.25" is used in the model, see Figures 3B.5-2 and 3B.5-3).

Finite Element Model

In order to calculate the buckling load, a three-dimensional ANSYS finite element model is constructed using a Shell 43 plastic large strain shell element. Shell 43 is well suited to model nonlinear, flat or warped, thin to moderately thick shell structures. The element has six degrees of freedom at each node: translations in the nodal x, y, and z directions and rotations about the nodal x, y, and z axes. The nodes at the locations of fusion welds are coupled for all degrees of freedom (the fusion welds rigidly connect the stainless steel boxes and stainless steel plates at these nodes). The nodes of various plates are coupled together in the out of plane direction so that they will bend in unison under surface pressure loading and to simulate the through thickness support provided by the poison plates. The finite element model is shown on Figure 3B.5-4.

Geometric Nonlinearities

Since the structure experiences large deformations before buckling, the large displacement option of ANSYS is used for all the analyses. The deflections during each load step are used to continuously redefine the geometry of the structure, thus producing a revised stiffness matrix. Therefore, buckling can be analyzed with the large deflection option. If the rate of change in deflection (per iteration) is observed, an estimation of the stability of the structure can be made. In particular, if the change of displacement at any node is increasing, the loading is above critical and the structure will eventually buckle.

Material Nonlinearities

The basket is constructed from 304 stainless steel. A bilinear stress strain relationship is used to simulate the correct nonlinear material behavior. The following elastic and inelastic material properties are used in the analysis:

Mechanical Properties of SA-240 Type 304 SS

	500°F	600°F
Modulus of Elasticity (psi)	25.8×10^6	25.3×10^6
Yield Strength (psi)	19,400	18,400
Ultimate Strength (psi)	63,500	63,400
Tangent Modulus (psi)	110,457	112,705

Loadings

The loadings on the panel model (Figure 3B.5-2, Location 1) were appropriately transferred from full size basket loadings. The loads used in 0, 10, 20, 30, and 45 degree drop analyses are summarized in the following table. Maximum loads of 200g were applied in each analysis. The automatic time stepping program option "Autots" was activated. This option lets the program decide the actual size of the load-substep for a converged solution. The program stops at the load substep when it fails to result in a converged solution. The last load step with a converged solution is the plastic instability load for the model. Figures 3B.5-5 shows the loading conditions.

Summary of Loads for Different Drop Orientations Analysis ($F_y = F \cos\theta$, $P_x = P \sin\theta$)

Drop Orientation (Degree)	1G load (12.25" Length) (Weight including all SS & poison plates above the bottom panel, rails, and 9 fuel assemblies**)		200 G Load Computer Run	
	Axial Load F_y (lb)	Trans. Load P_x (psi)	F_y (lb)	P_x (psi)
0	675	0	135,000	0
10	665	0.148	133,000	29.6
20	634	0.29	126,800	58.0
30	585	0.425	117,000	85
45	477	0.601	95,400	120.2

** This assumption is very conservative for drop orientation other than 0 degree, for example, for 30 and 45 degree drops the bottom panel only supports 7 fuel assemblies instead of 9 fuel assemblies.

Boundary Conditions

The ANSYS finite element model conservatively assumes that both ends of column are hinged. The boundary conditions are shown on Figure 3B.5-6. However, the stainless steel (0.3125" thick \times 1.75" wide) and poison plates forming the panel extend beyond the panel and connect into other panels so that moments can be developed at the top and bottom panel edges. These reactive end moments will keep the ends from rotating during buckling. Reference to "Formulas for Stress and Strain" by Raymond Roark⁽⁵⁾, Fourth Edition, Table XV indicates that:

Load Case No. (From Table XV of Roark)	Loading and Edge Condition	Formula for Critical Load (P)
2	End Load Both Ends Hinged	$P = (1)(\pi^2 EI/L^2)$
3	End Load Both Ends Fixed	$P = (4)(\pi^2 EI/L^2)$

Based on the formulas described above, the end conditions selected for the ANSYS model (both end hinged) are conservative and the calculated allowable compressive load has a large margin of safety.

3B.5.2 Analysis Results

ANSYS Finite Element Analysis Results

The plastic instability load and allowable buckling load for 0,10, 20, 30, and 45 degree orientation drops at 500°F and 600°F basket temperatures are summarized in the following tables. Based on the design criteria described in Section 3B.4.3, the allowable buckling load is equal to 70% of the calculated plastic instability load. Displacement and nodal stress intensity plots for 0, 10, 20, 30, and 45 degree orientation drops (500°F) at the last converged load step are shown on Figures 3B.5-7 through 3B.5-11.

Plastic Instability Load and Allowable Buckling Load

Drop Orientation (Degree)	Plastic Instability Load (G)	Allowable Buckling Load (G)
	Bottom Compartment At 500 °F (Location 1)	Bottom Compartment At 500 °F
0	153	107
10	144	100
20	139	97
30	138	96
45	144	100

Additional analysis is performed at location 2 (Figure 3B.5-2), conservatively using the same loading as in Location 1, based on 30 degree drop orientation (lowest allowable buckling load) and basket temperature of 600°F and the result is listed in the following table.

Plastic Instability Load and Allowable Buckling Load
(Figure 3B.5-2, Location 2)

Drop Orientation (Degree)	Plastic Instability Load, 600°F (G)	Allowable Buckling Load (G)
30	132	92

Result From Hand Calculation

As an order of magnitude check, the allowable buckling load based on 500°F temperature and 0 degree drop orientation is calculated below and compared to the ANSYS analysis results. As given in ASME⁽⁴⁾ Code, Subsection NF, Paragraph NF-3322-1(c)(2)(a)(Level A Condition) and modified as per Appendix F, Paragraph F-1334 (Level D Condition), the compressive stress limit for the accident condition (Level D) when KL/r is less than 120 and $S_u > 1.2 S_y$ is:

$$F_a = 2 \times S_y [0.47 - (KL/r)/444]$$

Where:

$$K = 0.65$$

$$L = 6.0''$$

$$S_y = 19,400 \text{ psi (at 500°F)}$$

$$S_u = 63,400 \text{ psi (at 500°F)}$$

$$I = b h^3/12 = 0.3038 \text{ in}^4$$

$$A = 5.12 \text{ in}^2$$

$$r = (I/A)^{1/2} = 0.2436 \text{ in}$$

$$KL/r = 0.65 \times 6.0/0.2436 = 16.1$$

Substituting the values given above,

$$F_a = 2 \times 19,400 [0.47 - (16.1)/444] = 16,829 \text{ psi}$$

The maximum allowable force is $16,829 \times 5.12 = 86,164 \text{ lb}$, therefore, the maximum allowable G load is:

$$G = 86,164 / 675 = 128$$

This value is reasonably close to the solution given by the ANSYS result (107 G).

3B.5.3 Evaluation

Based on the results of this analysis, it is concluded that the maximum allowable buckling load is 96g based on a stainless steel temperature of 500°F (Reference to Chapter 4, the maximum basket temperature at the outer basket panel is less than 471°F, therefore, use 500°F is conservative). This G load is higher than 77 G shown in the Appendix D cask impact analysis. The G load at the hottest part of the basket (595°F) is located at the center of the basket (see Chapter 4), the ANSYS run at this location (Figure 3B.5-2, location 2) based on 600°F temperature results in an allowable G load of 92. Therefore, the compressive and bending stresses developed in the stainless steel cannot cause the panel to buckle due to the tipover impact load.

3B.5.4 Analysis of the Aluminum Rails to Determine the Buckling Loads

The maximum membrane and bending stresses in the aluminum rails from the drop analyses (see Section 3B.4) at the most highly stressed location in the vertical member of the rail are listed below (1 G):

Location (Figure 3B.3-20)	Maximum Membrane S.I. (psi)	Maximum Bending S.I. (psi)
2 (Table 3B.3-2)	90	11**
3 (Table 3B.3-2)	51	8**

** These bending stress intensities are obtained through linearization of the cross section using ANSYS postprocessor

Criteria to Ensure Stability Under Compressive Loading

As given in ASME⁽⁴⁾ Code, Subsection NF, Paragraph NF-3322-1(c)(1)(a) and modified as per Appendix F, Paragraph F-1334, the compressive stress limit for the accident condition (Level D) when KL/r is less than C_c :

$$F_a = \frac{1.4 [1 - (KL/r)^2 / (2 C_c^2)] S_y}{5/3 + [3 (KL/r) / (8 C_c)] - [(KL/r)^3 / (8 C_c^3)]}$$

Where:

$$C_c = [(2 \pi^2 E) / S_y]^{1/2}$$

$$K = 1$$

$$L = 6.6" \text{ (location 2), } 4.8" \text{ (Location 3)}$$

$$S_y = 13,300 \text{ psi (at } 400^\circ\text{F)}$$

$$S_u = 16,000 \text{ psi (at } 400^\circ\text{F)}$$

$$E = 8.7 \times 10^6 \text{ (at } 400^\circ\text{F)}$$

$$I = b h^3 / 12 = 1(0.75)^3 / 12 = 0.0351 \text{ in}^4$$

$$A = 1.0 \times 0.75 = 0.75 \text{ in}^2$$

$$r = (I/A)^{1/2} = 0.216 \text{ in}$$

$$KL/r = 1 \times 6.6 / 0.216 = 30.55$$

$$C_c = [(2 \pi^2 \times 8.7 \times 10^6) / 13,300]^{1/2} = 113.63$$

$$F_a = \frac{1.4 [1 - (30.55)^2 / (2 \times 113.63^2)] (13,300)}{5/3 + [3 (30.55) / (8 \times 113.63)] - [(30.55)^3 / (8 \times 113.63^3)]} = 10,168 \text{ psi}$$

For $L = 4.8 \text{ in}$

$$KL/r = 1 \times 4.8 / 0.216 = 22.22$$

$$C_c = [(2 \pi^2 \times 8.7 \times 10^6) / 13,300]^{1/2} = 113.63$$

$$F_a = \frac{1.4 [1 - (22.22)^2 / (2 \times 113.63^2)] (13,300)}{5/3 + [3 (22.22) / (8 \times 113.63)] - [(22.22)^3 / (8 \times 113.63^3)]} = 10,502 \text{ psi}$$

Based on the above calculations, the allowable compressive stresses for the locations 2 & 3 are listed in the following table:

Location (Figure 3B.3-20)	Allowable Compressive Stress (F _a , psi)	Calculated Compressive Stress (1 G, psi)
2	10,168	90
3	10,502	51

Criteria To Prevent Failure Under Combined Loading (Compression + Bending)

For combined axial compression and bending, equations 20 and 21 of Paragraph NF-3322.1 (e) (1) apply.

$$f_a / F_a + C_{mx} (f_b) / (1 - f_a / F_e) F_b \leq 1.0 \text{ -----(1)}$$

and

$$f_a / (1.4)(0.6) S_y + f_b / F_b \leq 1.0 \text{ -----(2)}$$

The allowable stresses for the above equations are determined as follows:

	Allowable Stress	ASME Code Reference
F _a	10,168 psi (Location 2) 10,502 psi (Location 3)	NF-3322-1(c)(1)(a)
F _b	0.66 S _y ** = 8,788 psi	F-1334.5 (c)
C _{mx}	0.6	NF-3322.1 (e) (1) (b)
Note	The allowable stress F _a is multiplied by 1.4, which is the minimum factor allowed by Paragraph F-1334.	

** Conservatively use Level A allowable for Level D load calculations

The value of F_e is calculated by the formula below per Paragraph F-1334.5 (b):

$$F_e = \pi^2 (E) / (1.3) (KL/r)^2$$

Where:

K is conservatively taken as 1

L is the free length of the member, 6.6 in (Location 2), 4.8 in (Location 3)

r is the radius of gyration, in

E is the modulus of elasticity, 8.7×10^6 psi

This formula gives the following results for F_e :

Location	F_e (psi)
2 (L = 6.6", r = 0.216 in)	70,771
3 (L = 4.8", r = 0.216 in)	133,778

The interaction equations were evaluated based on:

Location 2 (Assume 100 g)

$$f_a / F_a + C_{mx} (f_b) / (1 - f_a / F_e) F_b = [(90 \times 100) / 10,168] + [0.6 \times (11 \times 100)] / [(1 - 90 \times 100 / 70,771) \times 8,778] = 0.971 \leq 1$$

$$f_a / (1.4)(0.6) S_y + f_b / F_b = [(90 \times 100) / (1.4 \times 0.6 \times 13,300)] + (11 \times 100) / 8,778 = 0.931 \leq 1$$

Location 3 (Assume 100 g)

$$f_a / F_a + C_{mx} (f_b) / (1 - f_a / F_e) F_b = [(51 \times 100) / 10,502] + [0.6 \times (8 \times 100)] / [(1 - 51 \times 100 / 133,778) \times 8,778] = 0.542 \leq 1$$

$$f_a / (1.4)(0.6) S_y + f_b / F_b = [(51 \times 100) / (1.4 \times 0.6 \times 13,300)] + [(8 \times 100) / 8,778] = 0.547 \leq 1$$

3B.5.5 Evaluation

Based on the result of this analysis, it concluded that the buckling load for aluminum rails is at

least 100 G under a side drop. This G load is much higher than the 77 G load shown on Appendix D cask impact analysis. Therefore, the compressive and bending stresses developed in the aluminum rails due to the tipover impact load cannot cause the rails to buckle.

3B.6 Summary of Basket Structural Analysis

3B.6.1 Stresses Due to Normal Condition Service

The following table summarized the normal condition basket structural analysis:

Stress Summary of Normal Condition Structural Analysis

Loading	Stress Category	Max. Stress (ksi)	Allowable Stress (ksi)	Reference Section/ Table
304 Stainless Steel Plate				
1G Lateral	P_m	0.36	14.76 ($S_m \times 0.9$)	Table 3B.3-1 (0° Drop)
	$P_m + P_b$	0.63	22.14 ($1.5 S_m \times 0.9$)	Table 3B.3-1 (0° Drop)
3G Vertical	P_m	0.30	14.76 ($S_m \times 0.9$)	Sect. 3B.3.3
Stainless Steel Fusion Weld				
1G Lateral	τ	0.055	2.95 ($0.6 S_m \times 0.3$)	Table 3B.3-1 (45° Drop)
3G Vertical	τ	0.05	2.95 ($0.6 S_m \times 0.3$)	Sect. 3B.3.3
6061-T6 Aluminum Rail				
1G Lateral	P_m	0.11	4.5 (S_m)	Table 3B.3-2 (Location 1)
	$P_m + P_b$	0.15	6.75 ($1.5 S_m$)	Table 3B.3-2 (Location 1)
3G Vertical	P_m	0.05	4.5 (S_m)	Sect. 3B.3.3

Based on the results shown on the above table, all of the calculated stresses in the basket and rails are acceptable.

3B.6.2 Stresses Due to Accident Condition

The following table summarized the accident condition basket structural analysis:

Stress Summary of Accident Condition Structural Analysis

Loading	Stress Category	Max. Stress (ksi)	Allowable Stress (ksi)	Max. Allowable G load	Max. Calculated G Load	Reference Section/Table
304 Stainless Steel Plate						
60 G End Drop	P_m	6.03 (60G)	39.36 (2.4 S_m)	392	60	Sect. 3B.4.1
Side drop Stress Analysis	P_m	0.36 (1G)	39.36 (2.4 S_m)	109	77	Table 3B.4-1 (0° drop)
	$P_m + P_b$	0.63 (1G)	59.04 (S_u)	94	77	Table 3B.4-1 (0° drop)
Side drop Buckling Analysis				92	77	Sect. 3B.5.2
Stainless Steel Fusion weld						
60 G End Drop	τ	0.92 (60G)	19.68 (0.6 $S_m \times 2$)	1283	60	Sect. 3B.4.1
Side Drop Stress Analysis	τ	0.055 (1G)	19.68 (0.6 $S_m \times 2$)	358	77	Table 3B.4-1 (45° drop)
6061-T6 Aluminum Rail						
60 G End Drop	P_m	1.0 (60G)	10.8 (2.4 S_m)	648	60	Sect. 3B.4.1
Side Drop Stress analysis	P_m	0.11 (1G)	10.8 (2.4 S_m)	98	77	Table 3B.4-2 (Location 1)
	$P_m + P_b$	0.15 (1G)	16.0 (S_u)	107	77	Table 3B.4-2 (Location 1)
Side Impact Buckling Analysis				100	77	Sect. 3B.5.4

Based on this analysis, the basket and rails are structurally adequate up to 94 G (limited by 0° side drop), this G load is higher than the calculated G load of 77 from tip over impact analysis described in Appendix D. The basket and rails will remain in place and maintain separation of adjacent fuel assemblies.

3B.7 References

1. ANSYS Engineering Analysis System User's Manual, Rev. 6.0, 2001. |
2. ASME B&PV Code, Section II, Part D, 1998 including 2000 Addendum. |
3. ASME B&PV Code, Section III Appendices and Subsection NG, 1995 including 1996 Addendum.
4. ASME B&PV Code, Section III, Subsection NF, 1995 including 1996 Addendum.
5. Roark, R. "Formulas for Stress and Strain" Fourth Edition.
6. ASME B&PV Code, Section III, Appendix F, 1995 including 1996 Addendum. |

Table 3B.3-1
Summary of Basket Stress Analysis - Normal Condition
(1G Side Load)

Drop Orientation (Degree)	Component	Stress Category	Max. Stress (1G) (ksi)	Allowable Stress (ksi)	Reference Figures
0	S.S. Plate	P_m	0.24	14.76	3B.3-4
		$P_m + P_b$	0.63	22.14	3B.3-5
	S.S. Box	P_m	0.36	14.76	3B.3-6
		$P_m + P_b$	0.38	22.14	3B.3-7
	Fusion Weld	τ	0.043	2.95	Fig. 3B.3-23
30	S.S. Plate	P_m	0.21	14.76	3B.3-8
		$P_m + P_b$	0.47	22.14	3B.3-9
	S.S. Box	P_m	0.28	14.76	3B.3-10
		$P_m + P_b$	0.35	22.14	3B.3-11
45	S.S. Plate	P_m	0.17	14.76	3B.3-12
		$P_m + P_b$	0.40	22.14	3B.3-13
	S.S. Box	P_m	0.23	14.76	3B.3-14
		$P_m + P_b$	0.31	22.14	3B.3-15
	Fusion Weld	τ	0.055	2.95	Fig. 3B.3-24

Table 3B.3-2
Linearized Stress Intensities of Aluminum Rail - Normal Condition
(0° Side Load)

Location (Figures 3B.3-20 &21)	Stress Category	Max. S.I. 1G (ksi)	Allowable S.I. (ksi)
1	P_m	0.11	4.5
	$P_m + P_b$	0.15	6.75
2	P_m	0.09	4.5
	$P_m + P_b$	0.10	6.75
3	P_m	0.05	4.5
	$P_m + P_b$	0.06	6.75
4	P_m	0.02	4.5
	$P_m + P_b$	0.03	6.75
5	P_m	0.01	4.5
	$P_m + P_b$	0.02	6.75

Table 3B.3-3
Linearized Stress Intensities of Aluminum Rail - Normal Condition
(30° Side Load)

Location (Figures 3B.3-20 &21)	Stress Category	Max. S.I. 1G (ksi)	Allowable S.I. (ksi)
1	P_m	0.08	4.5
	$P_m + P_b$	0.11	6.75
2	P_m	0.08	4.5
	$P_m + P_b$	0.09	6.75
3	P_m	0.04	4.5
	$P_m + P_b$	0.05	6.75
4	P_m	0.03	4.5
	$P_m + P_b$	0.03	6.75
5	P_m	0.02	4.5
	$P_m + P_b$	0.02	6.75

Table 3B.3-4
Linearized Stress Intensities of Aluminum Rail - Normal Condition
(45° Side Load)

Location (Figures 3B.3- 20&21)	Stress Category	Max. S.I. 1G (ksi)	Allowable S.I. (ksi)
1	P_m	0.06	4.5
	$P_m + P_b$	0.08	6.75
2	P_m	0.06	4.5
	$P_m + P_b$	0.07	6.75
3	P_m	0.04	4.5
	$P_m + P_b$	0.04	6.75
4	P_m	0.02	4.5
	$P_m + P_b$	0.02	6.75
5	P_m	0.02	4.5
	$P_m + P_b$	0.03	6.75

Table 3B.4-1
Summary of Basket Stress Analysis - Accident Condition
(Side Drop)

Drop Orientation (Degree)	Component	Stress Category	Max. Stress (1G) (ksi)	Allowable Stress (ksi)	Max. Allowable G Load
0	S.S. Plate	P_m	0.24	39.36	164
		$P_m + P_b$	0.63	59.04	94
	S.S. Box	P_m	0.36	39.36	109
		$P_m + P_b$	0.38	59.04	155
	Fusion Weld	τ	0.043	19.68	458
30	S.S. Plate	P_m	0.21	39.36	187
		$P_m + P_b$	0.47	59.04	126
	S.S. Box	P_m	0.28	39.36	141
		$P_m + P_b$	0.35	59.04	169
45	S.S. Plate	P_m	0.17	39.36	232
		$P_m + P_b$	0.40	59.04	148
	S.S. Box	P_m	0.23	39.36	171
		$P_m + P_b$	0.231	59.04	256
	Fusion Weld	τ	0.055	19.68	358

Table 3B.4-2
Linearized Stress Intensities of Aluminum Rail - Accident Condition
(0° Side Drop)

Location (Figures 3B.3-20 &21)	Stress Category	Max. S.I. 1G (ksi)	Allowable S.I. (ksi)	Max. Allowable G Loads
1	P_m	0.11	10.8	98
	$P_m + P_b$	0.15	16.0	107
2	P_m	0.09	10.8	120
	$P_m + P_b$	0.10	16.0	160
3	P_m	0.05	10.8	216
	$P_m + P_b$	0.06	16.0	267
4	P_m	0.02	10.8	540
	$P_m + P_b$	0.03	16.0	533
5	P_m	0.01	10.8	1080
	$P_m + P_b$	0.02	16.0	800

Table 3B.4-3
Linearized Stress Intensities of Aluminum Rail - Accident Condition
(30° Side Drop)

Location (Figures 3B.3-20 &21)	Stress Category	Max. S.I. 1G (ksi)	Allowable S.I. (ksi)	Max. Allowable G Loads
1	P_m	0.08	10.8	135
	$P_m + P_b$	0.11	16.0	146
2	P_m	0.08	10.8	135
	$P_m + P_b$	0.09	16.0	178
3	P_m	0.04	10.8	270
	$P_m + P_b$	0.05	16.0	320
4	P_m	0.03	10.8	360
	$P_m + P_b$	0.03	16.0	533
5	P_m	0.02	10.8	540
	$P_m + P_b$	0.02	16.0	800

Table 3B.4-4
Linearized Stress Intensities of Aluminum Rail - Accident Condition
(45° Side Drop)

Location (Figures 3B.3-20 &21)	Stress Category	Max. S.I. 1G (ksi)	Allowable S.I. (ksi)	Max. Allowable G Loads
1	P_m	0.06	10.8	180
	$P_m + P_b$	0.08	16.0	200
2	P_m	0.06	10.8	180
	$P_m + P_b$	0.07	16.0	229
3	P_m	0.04	10.8	270
	$P_m + P_b$	0.04	16.0	400
4	P_m	0.02	10.8	540
	$P_m + P_b$	0.02	16.0	800
5	P_m	0.02	10.8	540
	$P_m + P_b$	0.03	16.0	533

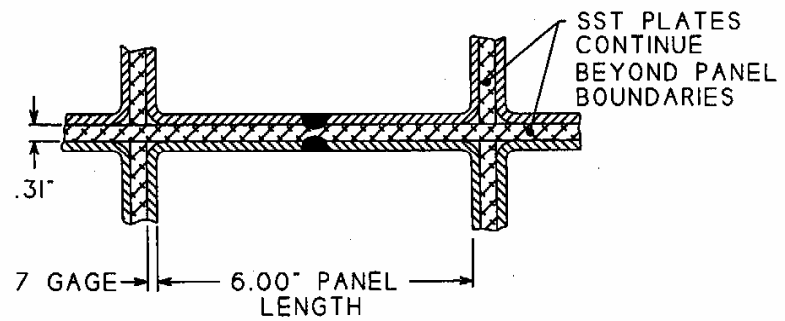
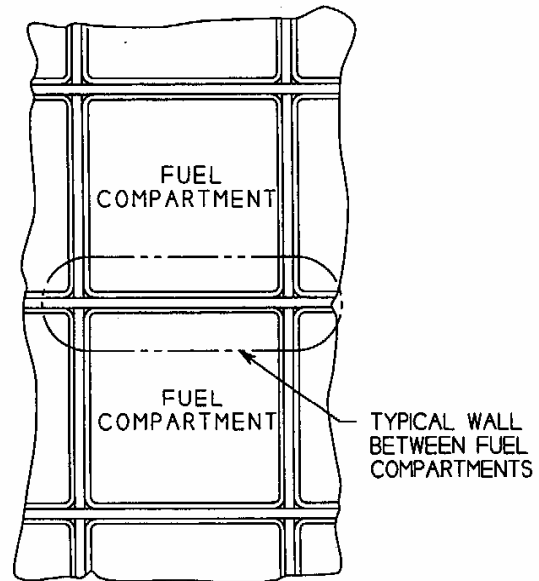


Figure 3B.1-1
REPRESENTATIVE BASKET
WALL PANEL

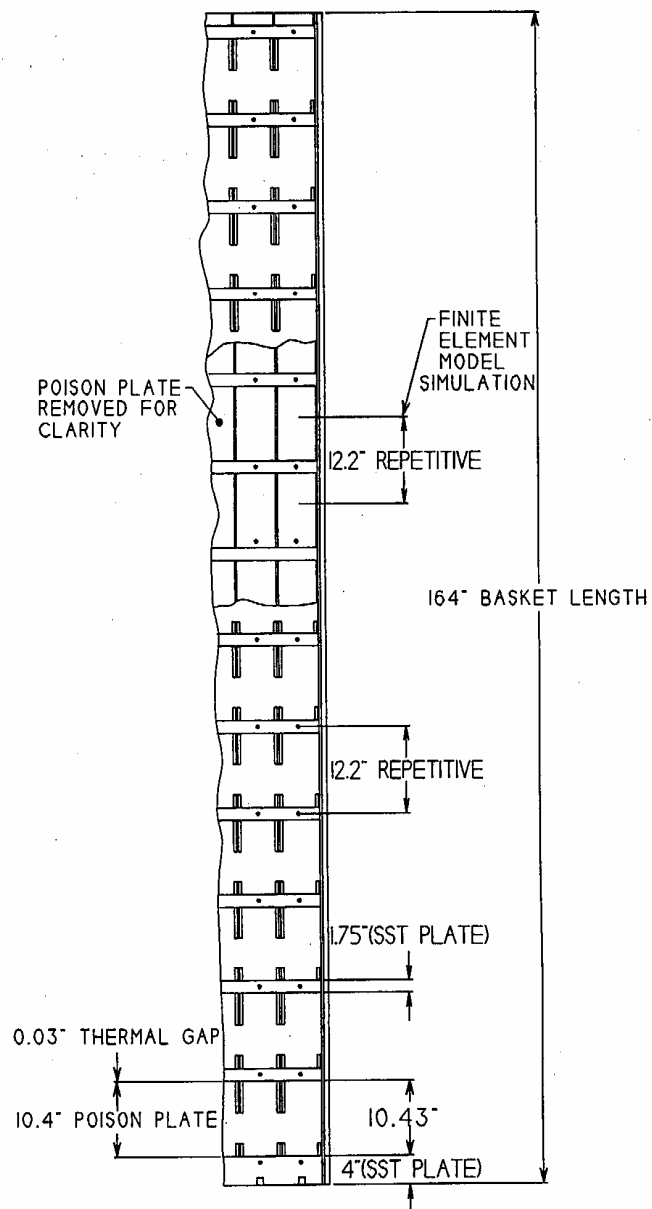


FIGURE 3B.2-1
AXIAL VIEW OF BASKET

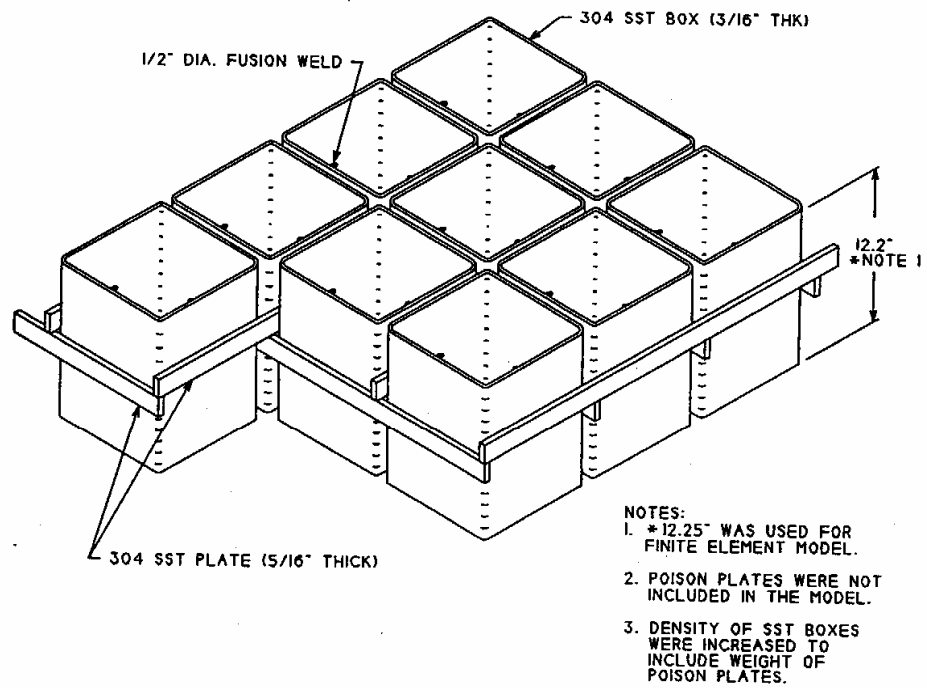


FIGURE 3B.2-2
GEOMETRY FOR ANSYS
MODEL

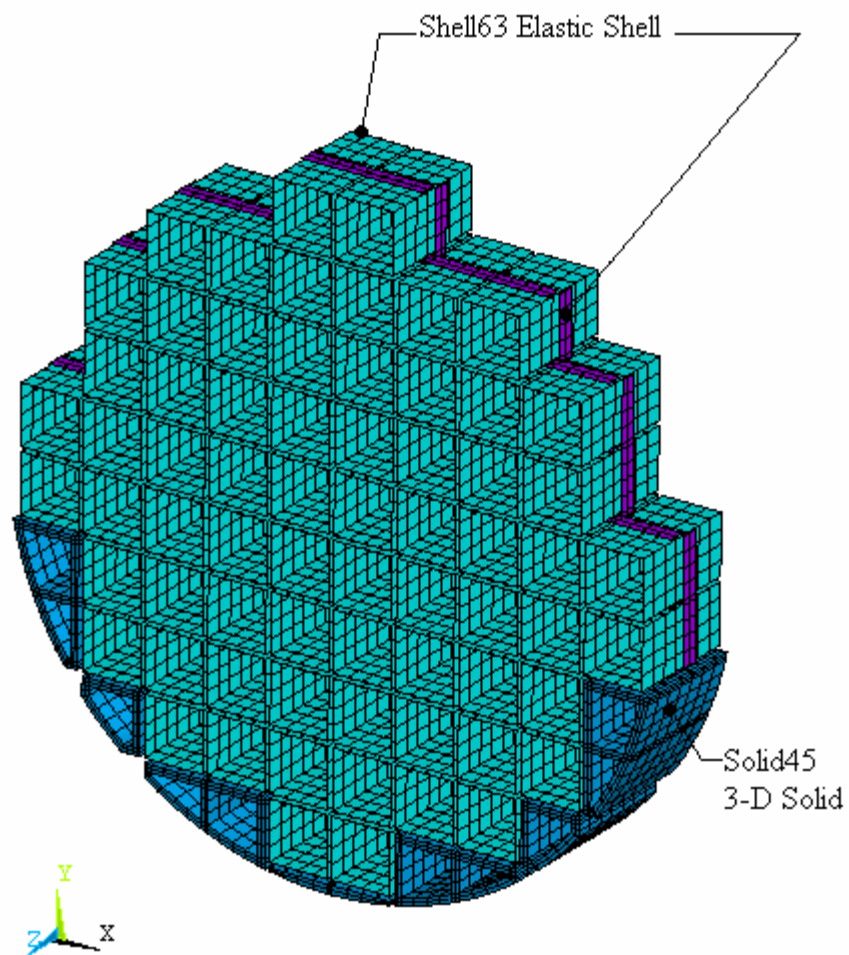


FIGURE 3B.2-3
FINITE ELEMENT MODEL AND
ELEMENT TYPES

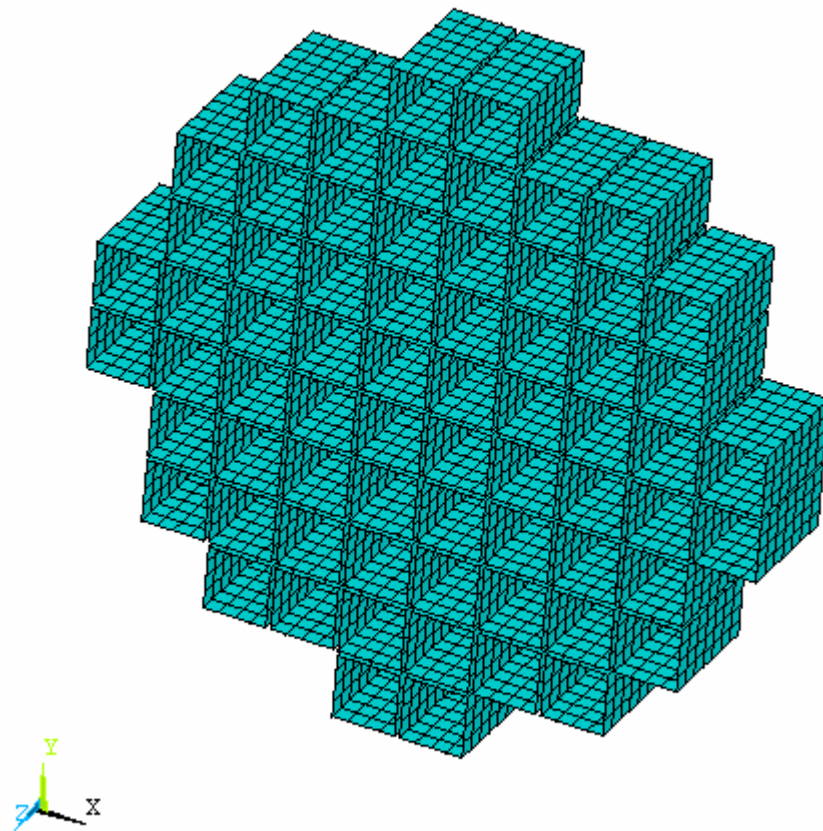


FIGURE 3B.2-4
BASKET FINITE ELEMENT
MODEL- STAINLESS STEEL
BOXES

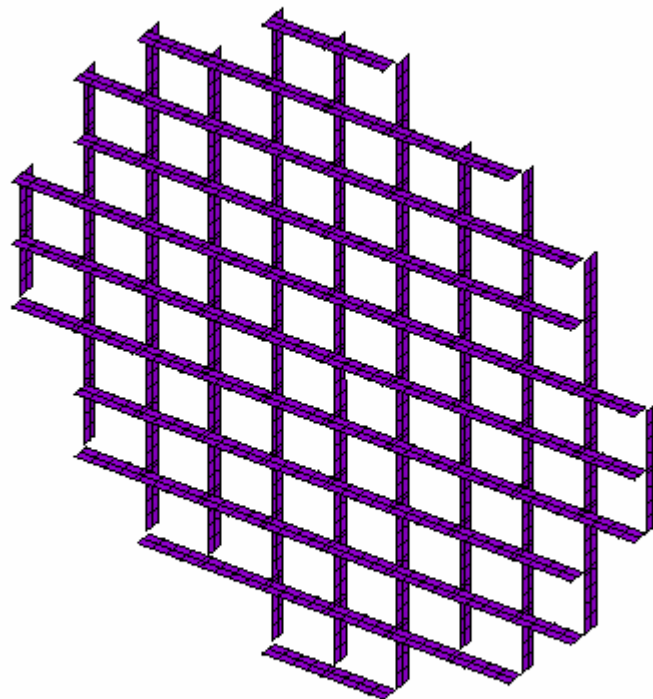


FIGURE 3B.2-5
BASKET FINITE ELEMENT
MODEL- STAINLESS STEEL
PLATES

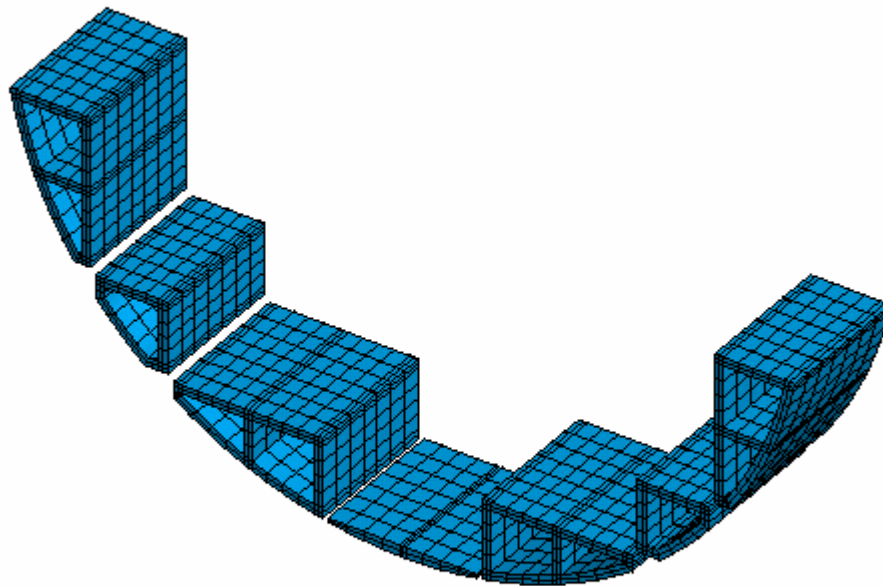


FIGURE 3B.2-6
BASKET FINITE ELEMENT
MODEL-ALUMINUM RAILS

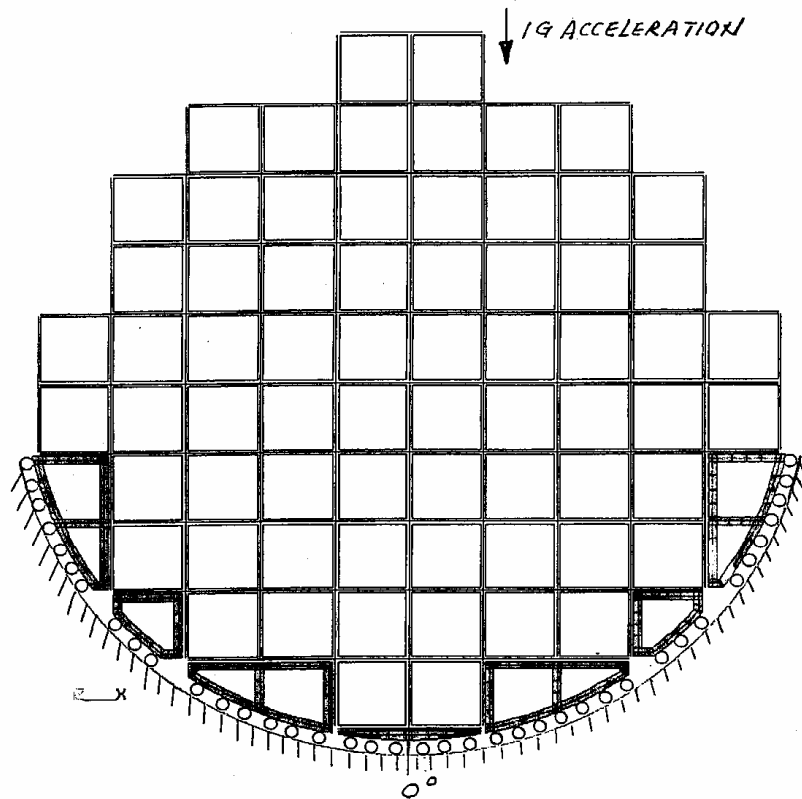


FIGURE 3B.3-1
LOADING AND BOUNDARY
CONDITIONS-0° DROP

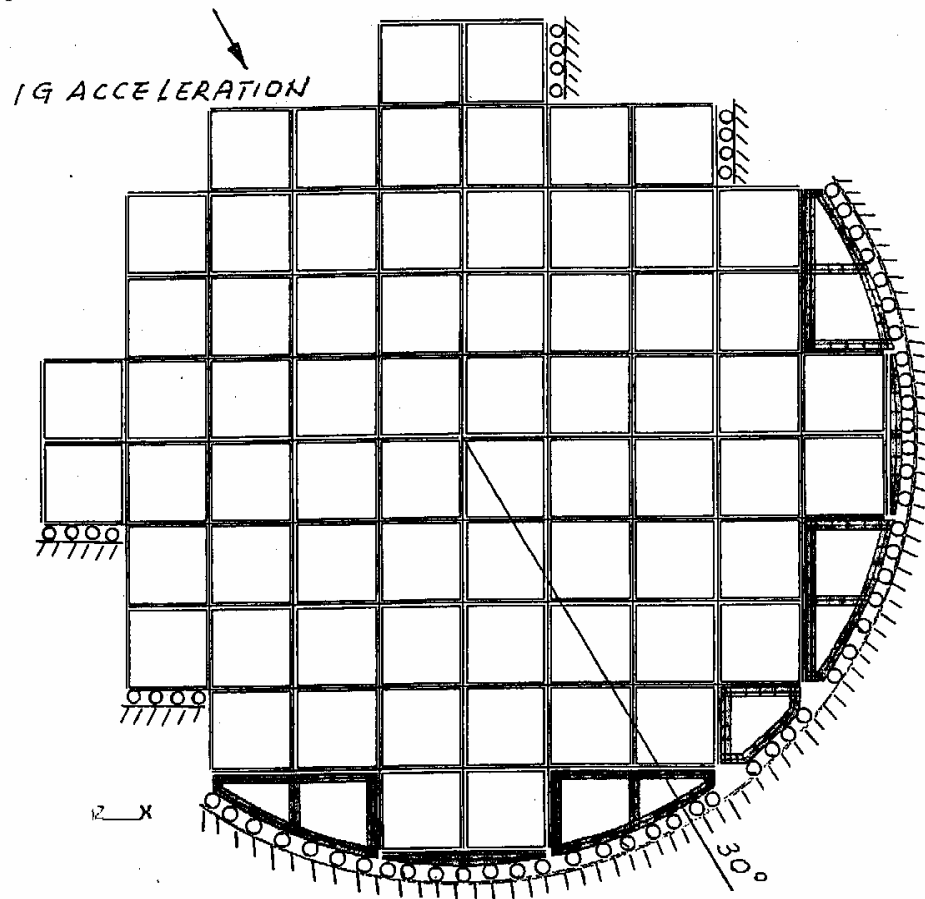


FIGURE 3B.3-2
LOADING AND BOUNDARY
CONDITIONS-30° DROP

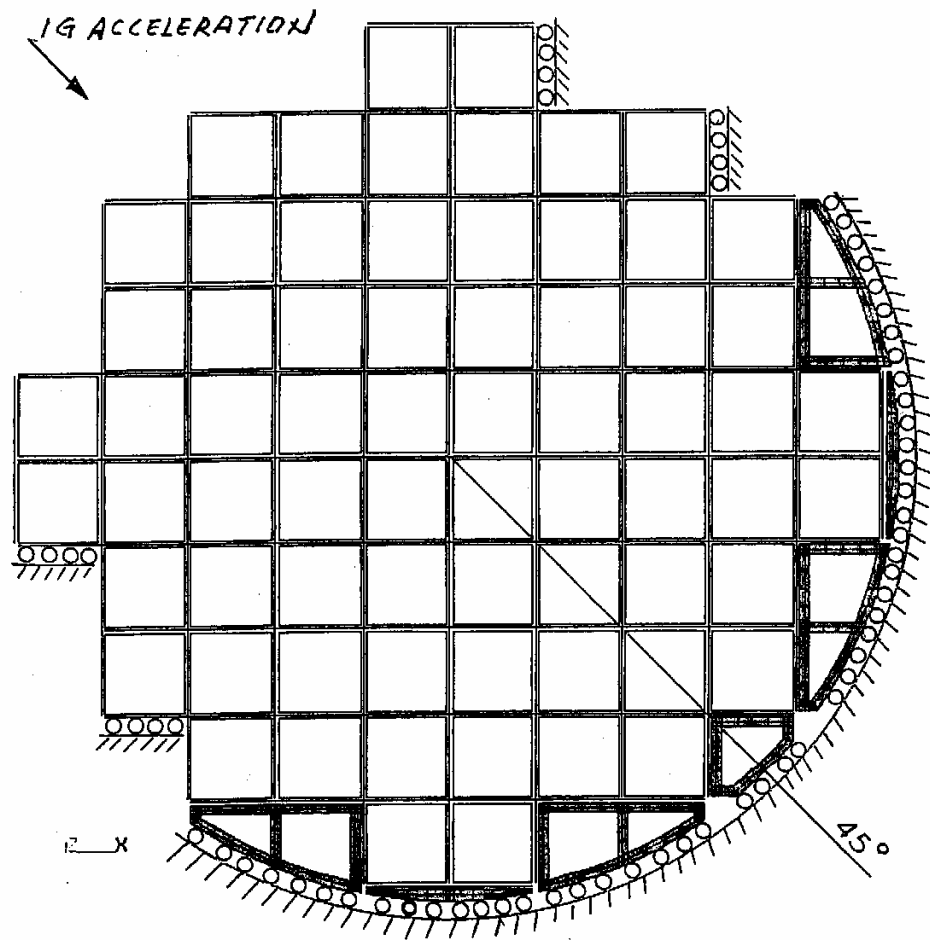


FIGURE 3B.3-3
LOADING AND BOUNDARY
CONDITIONS-45° DROP

Figure 3B.3-4
Membrane Stress Intensity (SS Plate)-0 Degree Drop

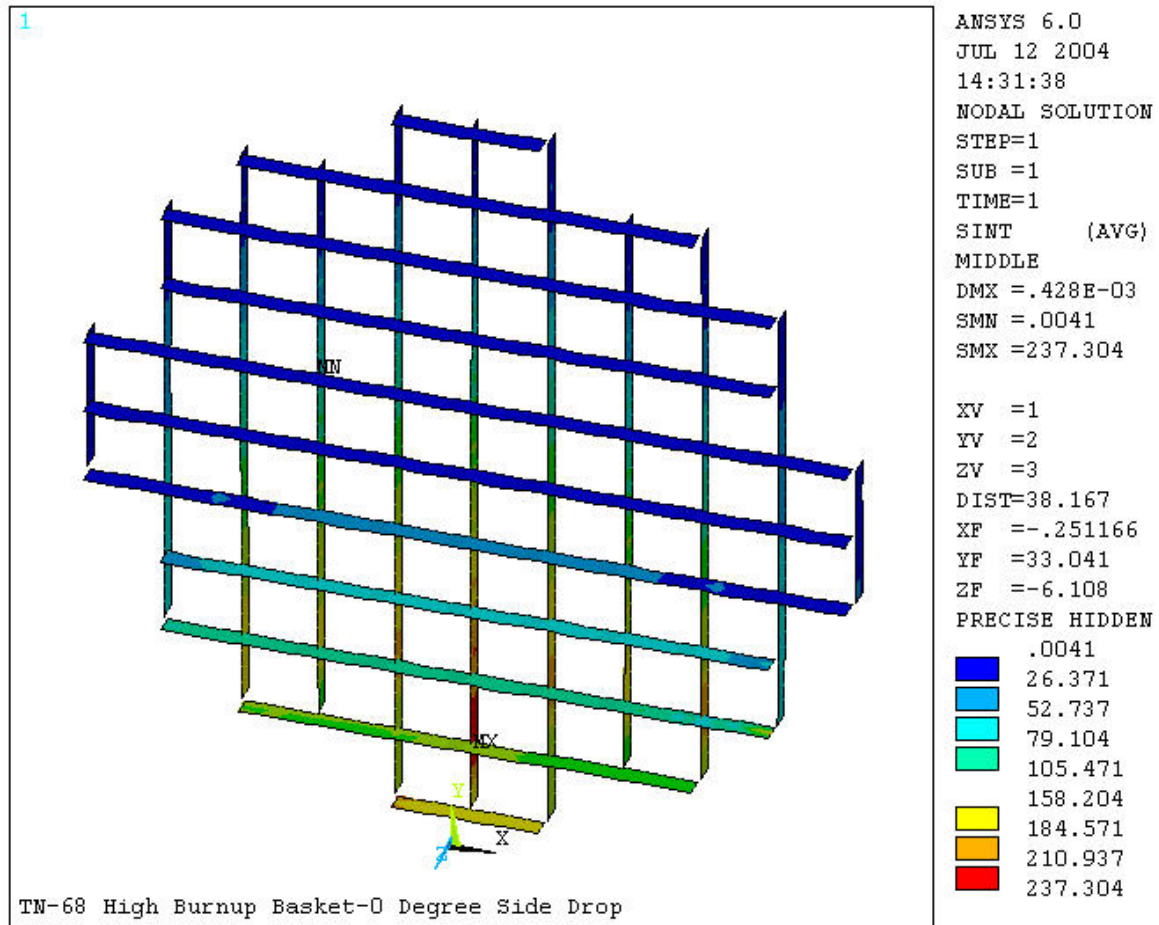


Figure 3B.3-5
Membrane + Bending Stress Intensity (SS Plate)-0 degree Drop

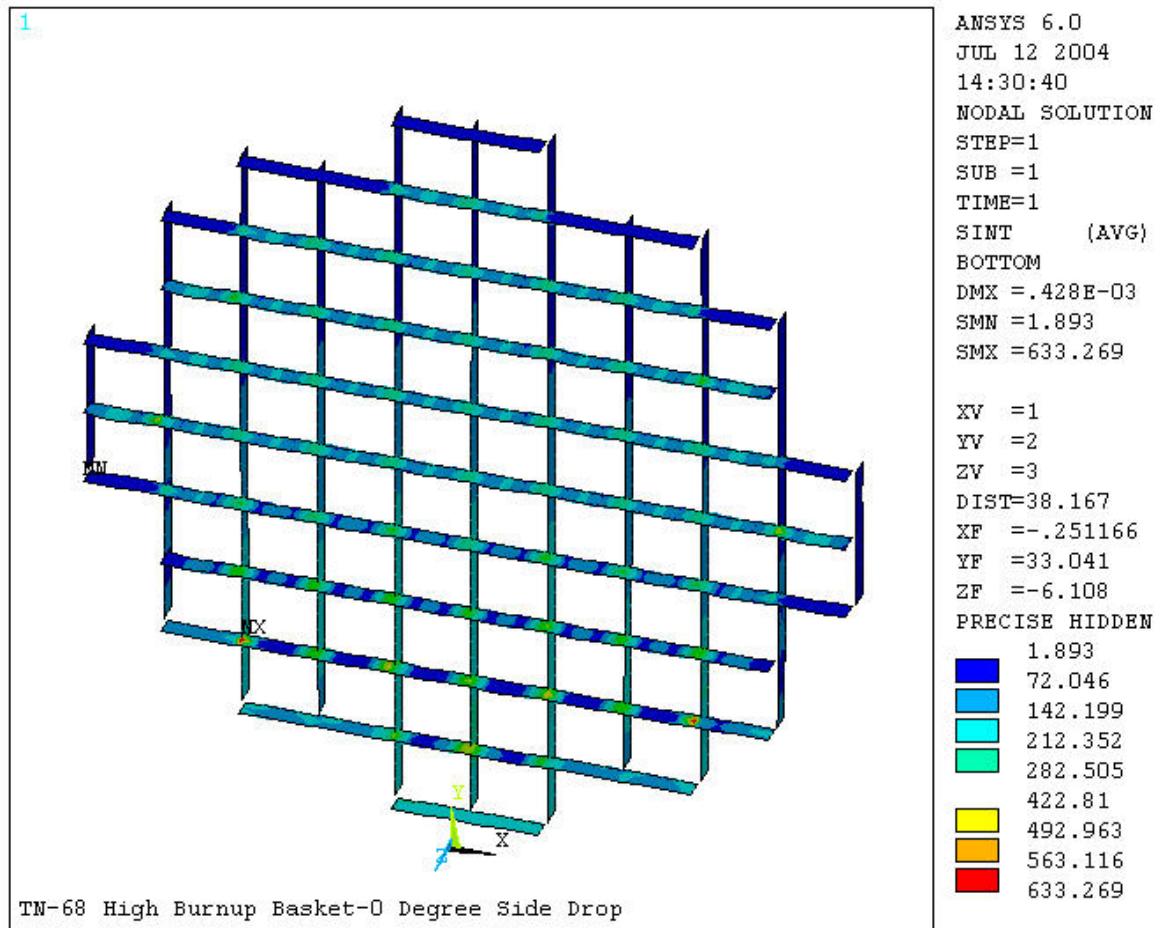


Figure 3B.3-6
Membrane Stress Intensity (SS Box)-0 Degree Drop

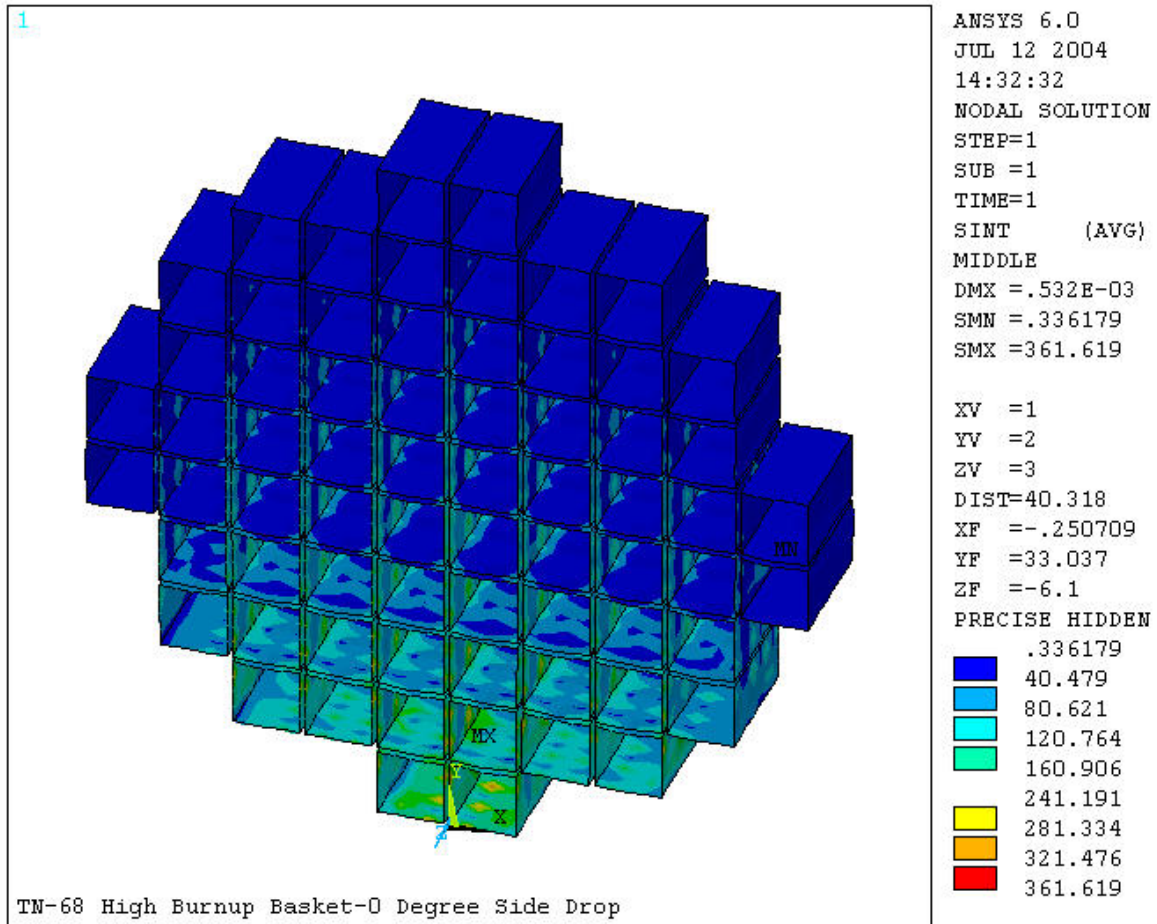


Figure 3B.3-7
Membrane + Bending Stress Intensity (SS Box)-0 Degree Drop

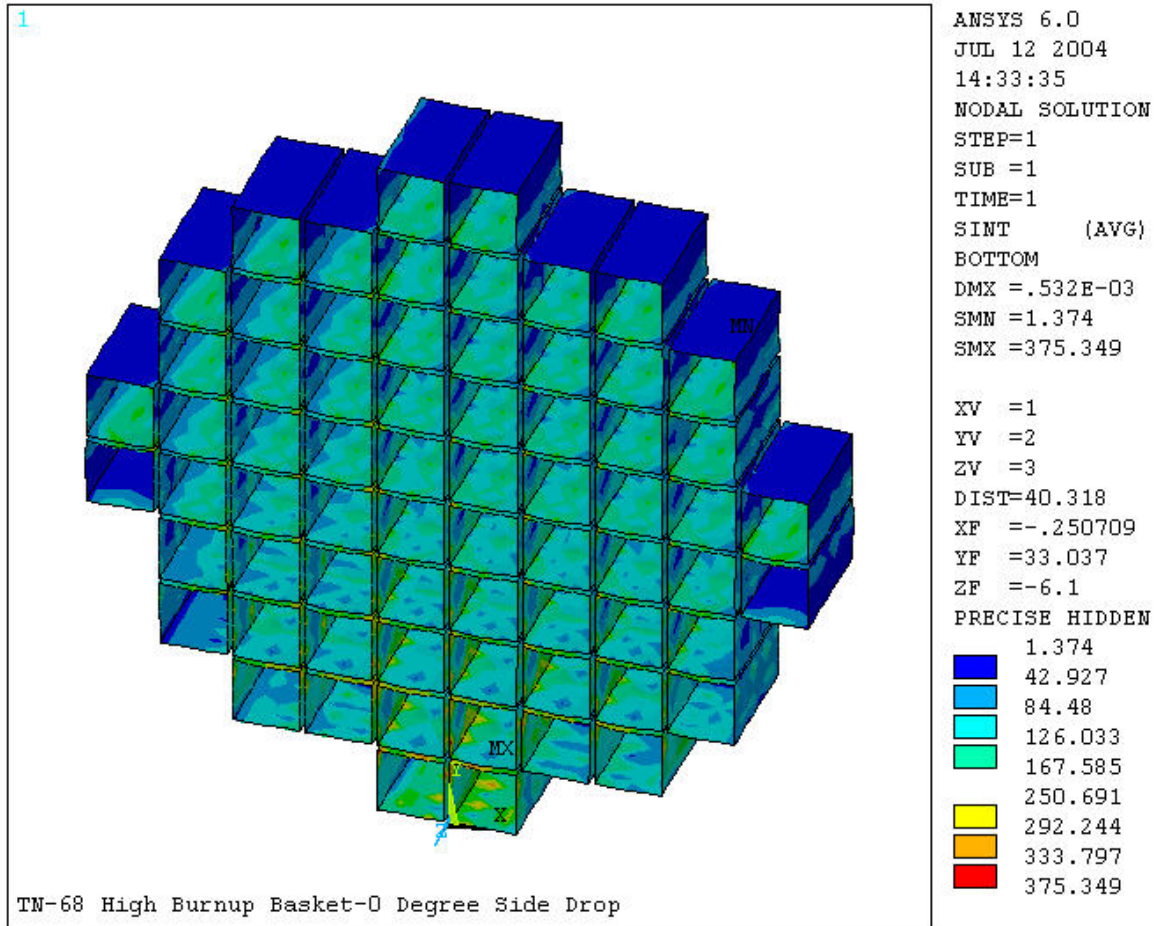


Figure 3B.3-8
Membrane Stress Intensity (SS Plate)-30 Degree Drop

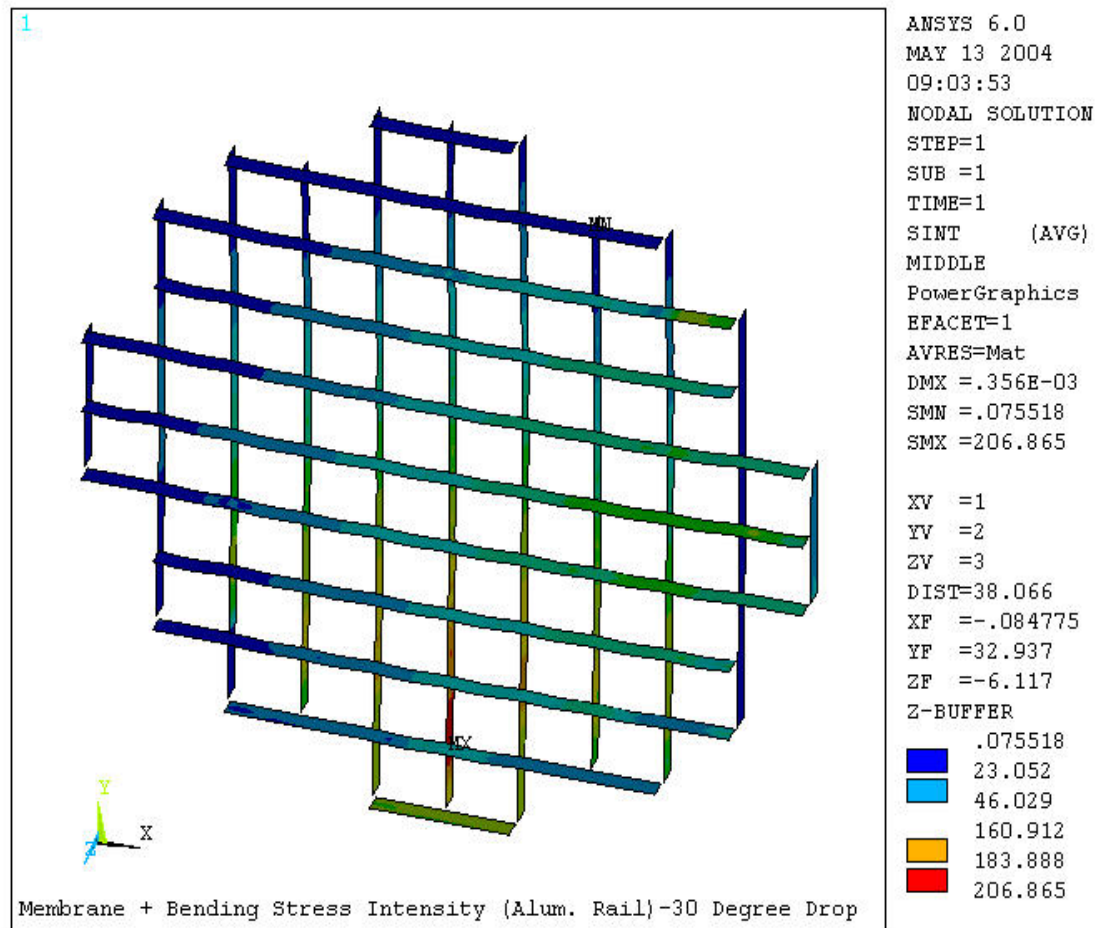


Figure 3B.3-9
Membrane + Bending Stress Intensity (SS Plate)-30 degree Drop

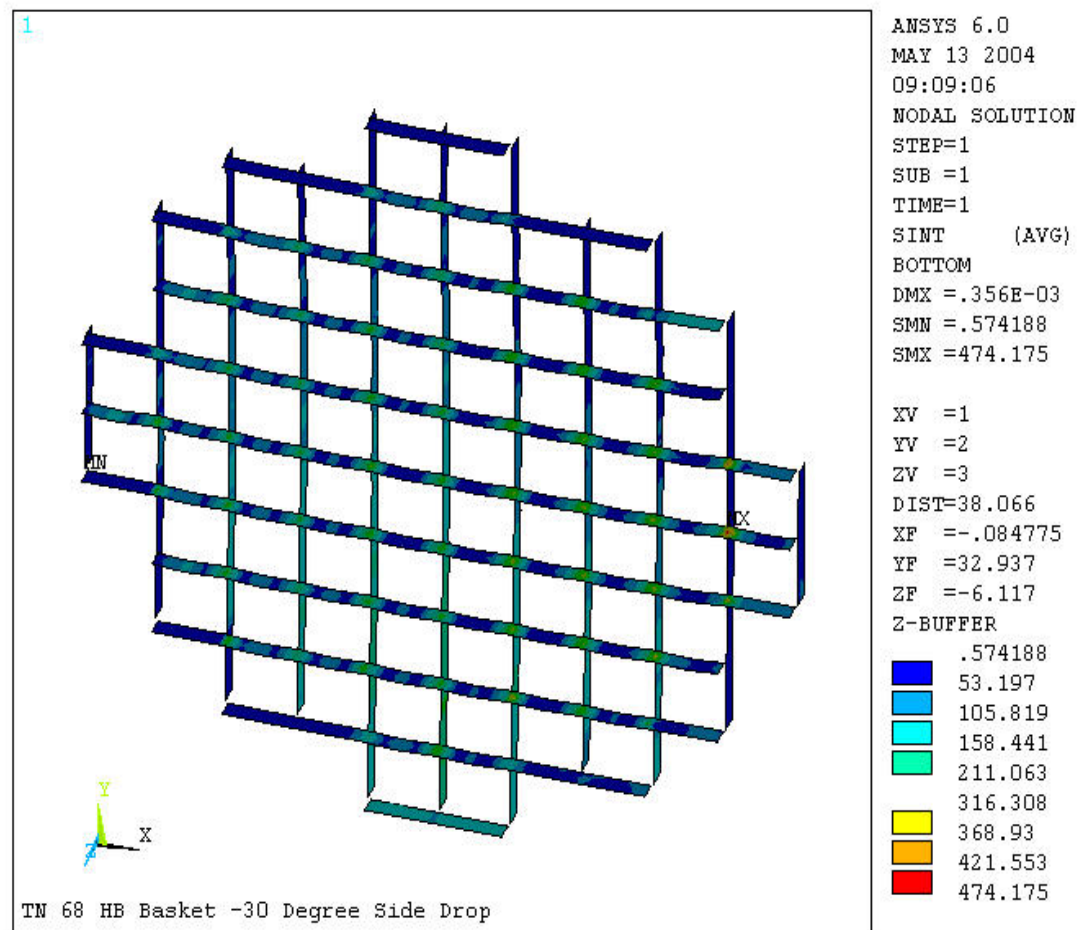


Figure 3B.3-10
Membrane Stress Intensity (SS Box)-30 Degree Drop

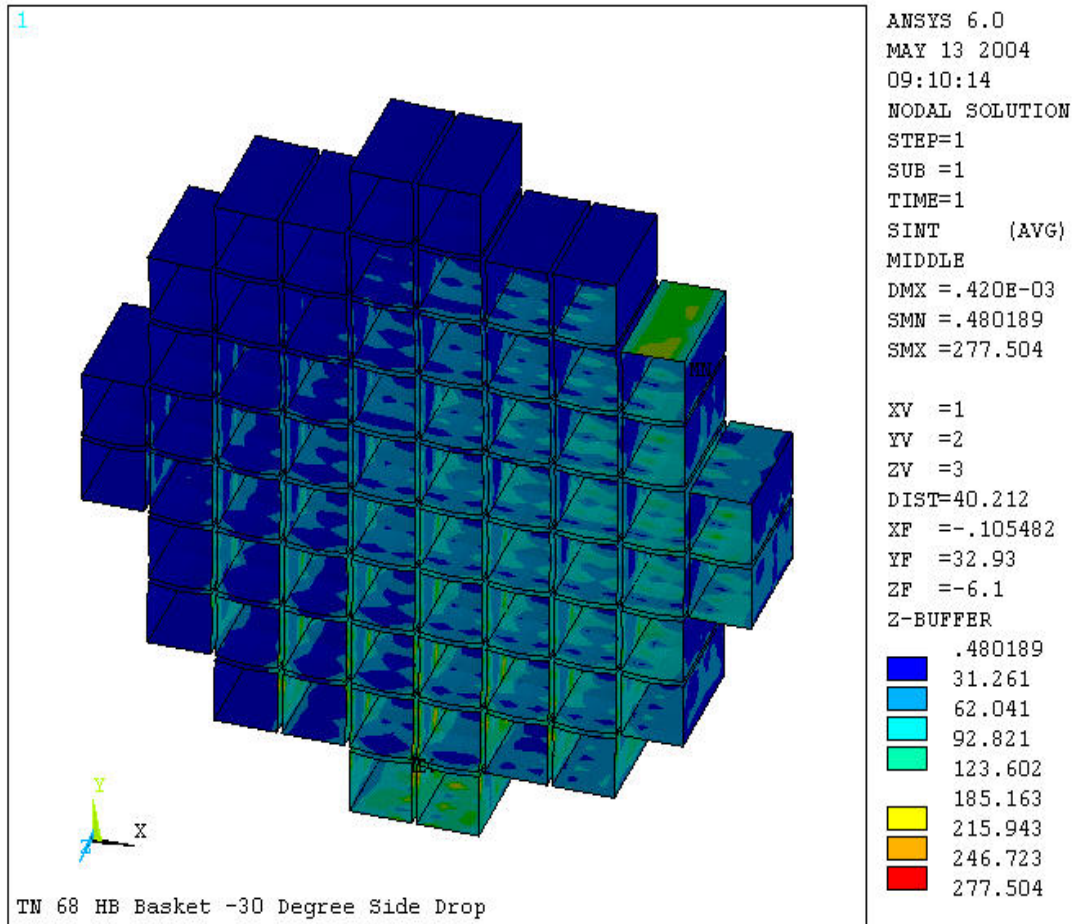


Figure 3B.3-11
Membrane + Bending Stress Intensity (SS Box)-30 Degree Drop

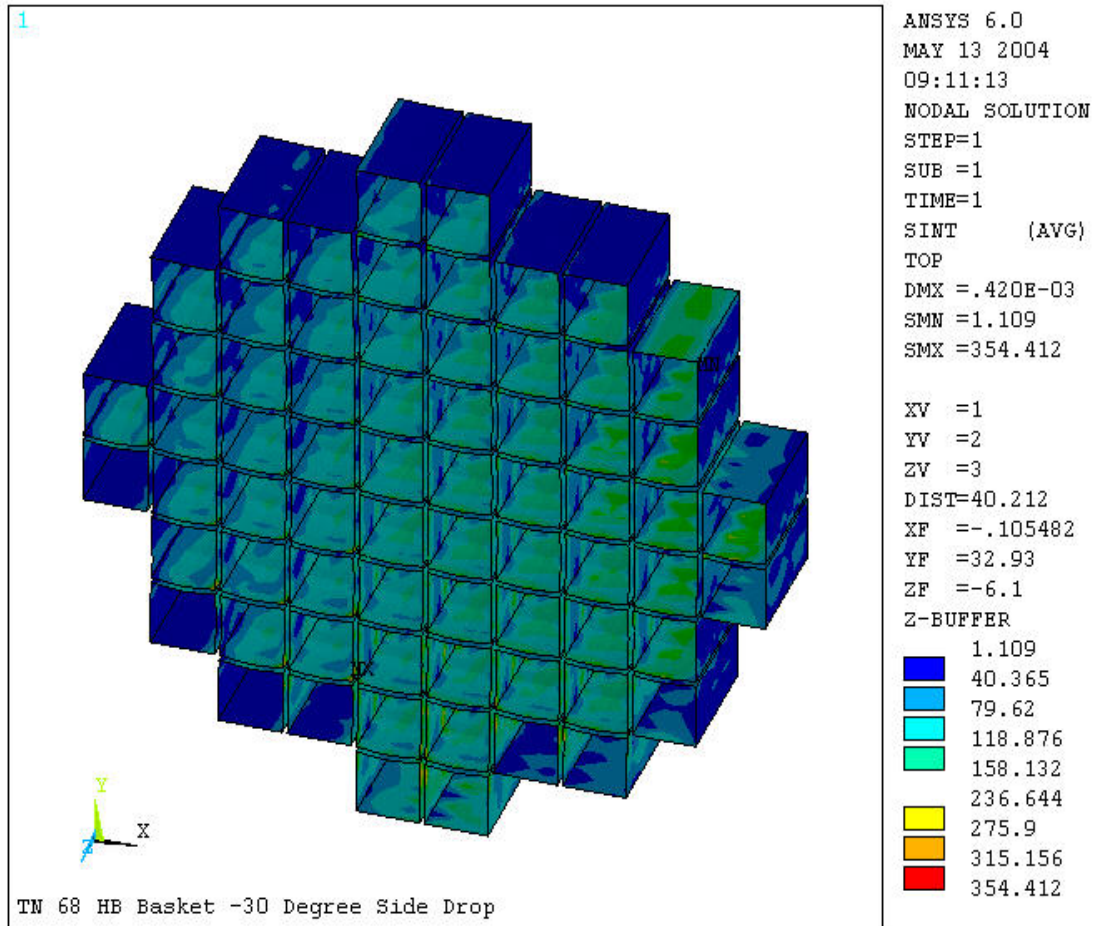


Figure 3B.3-12
Membrane Stress Intensity (SS Plate)-45 Degree Drop

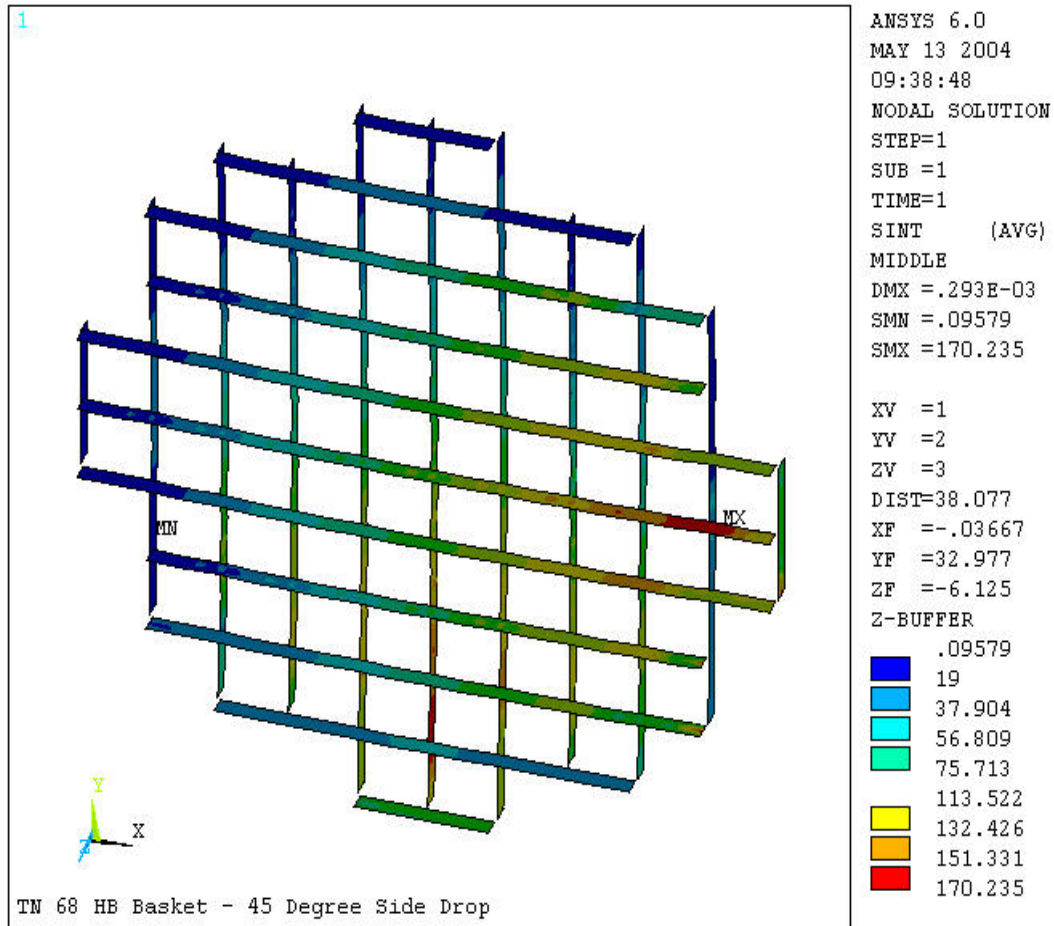


Figure 3B.3-13
 Membrane + Bending Stress Intensity (SS Plate)-45 Degree Drop

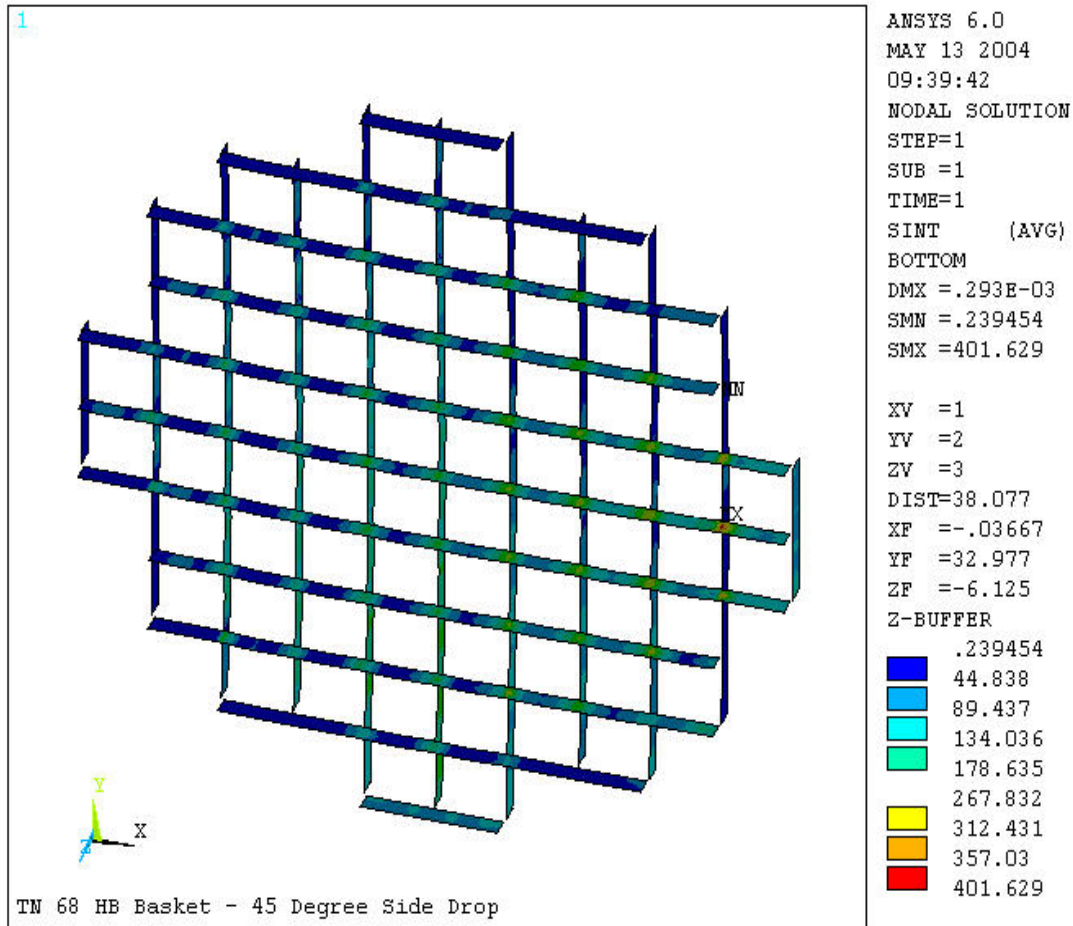


Figure 3B.3-14
Membrane Stress Intensity (SS Box)-45 Degree Drop

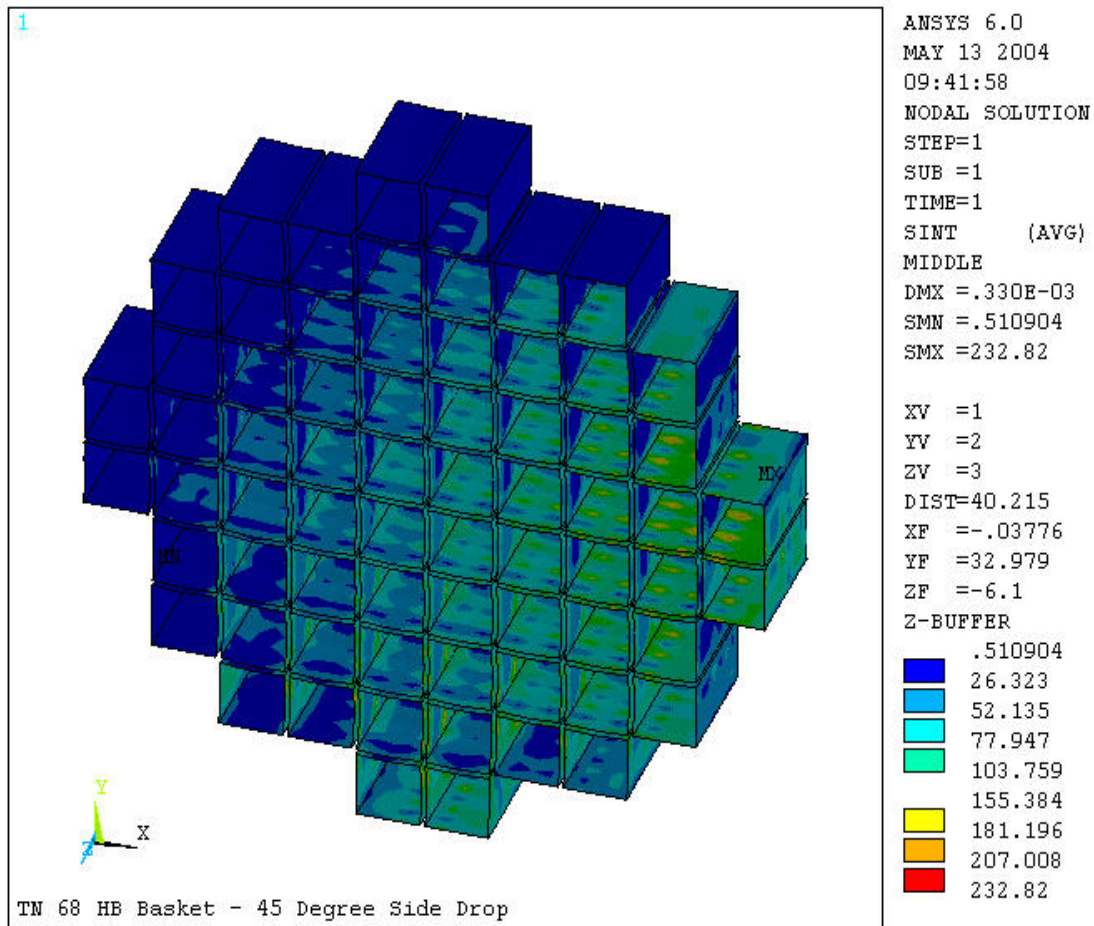


Figure 3B.3-15
Membrane + Bending Stress Intensity (SS Box)-45 Degree Drop

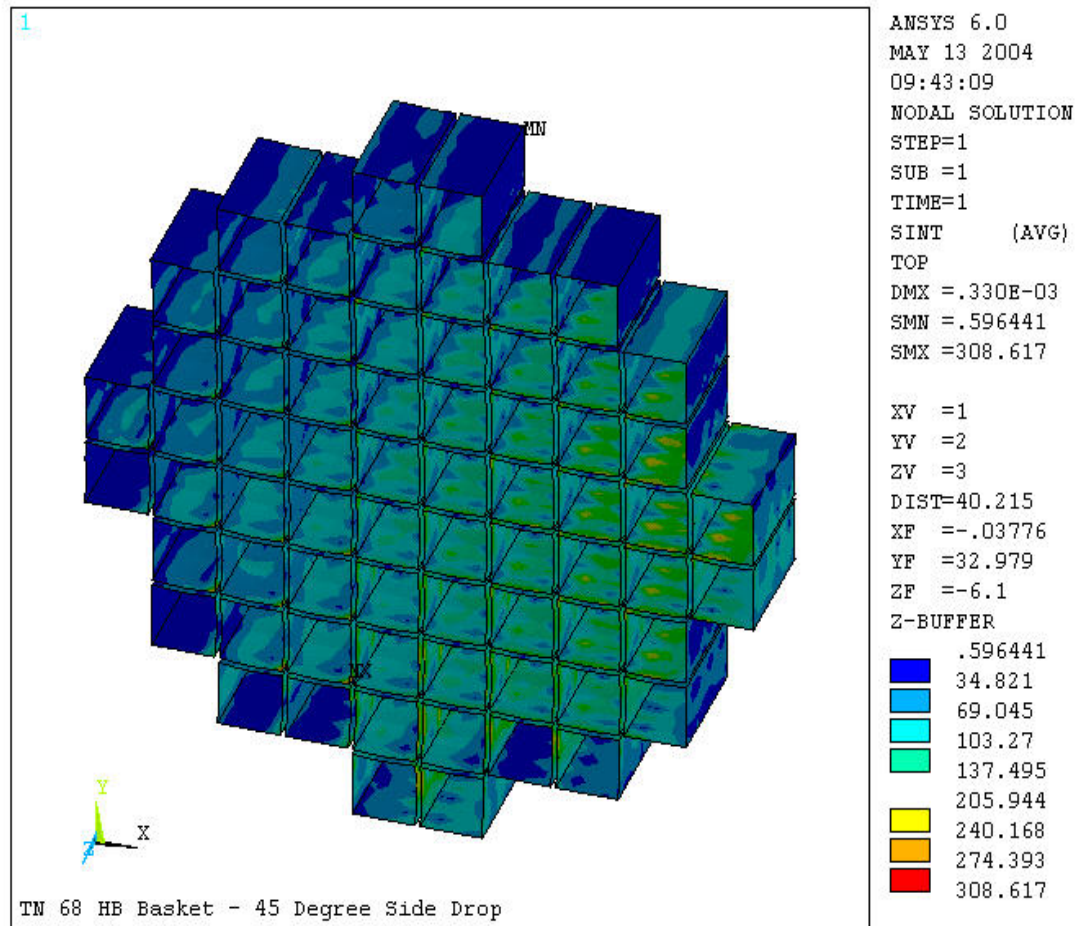


Figure 3B.3-16
Nodal Stress Intensity (Aluminum Rails)-0 Degree Drop

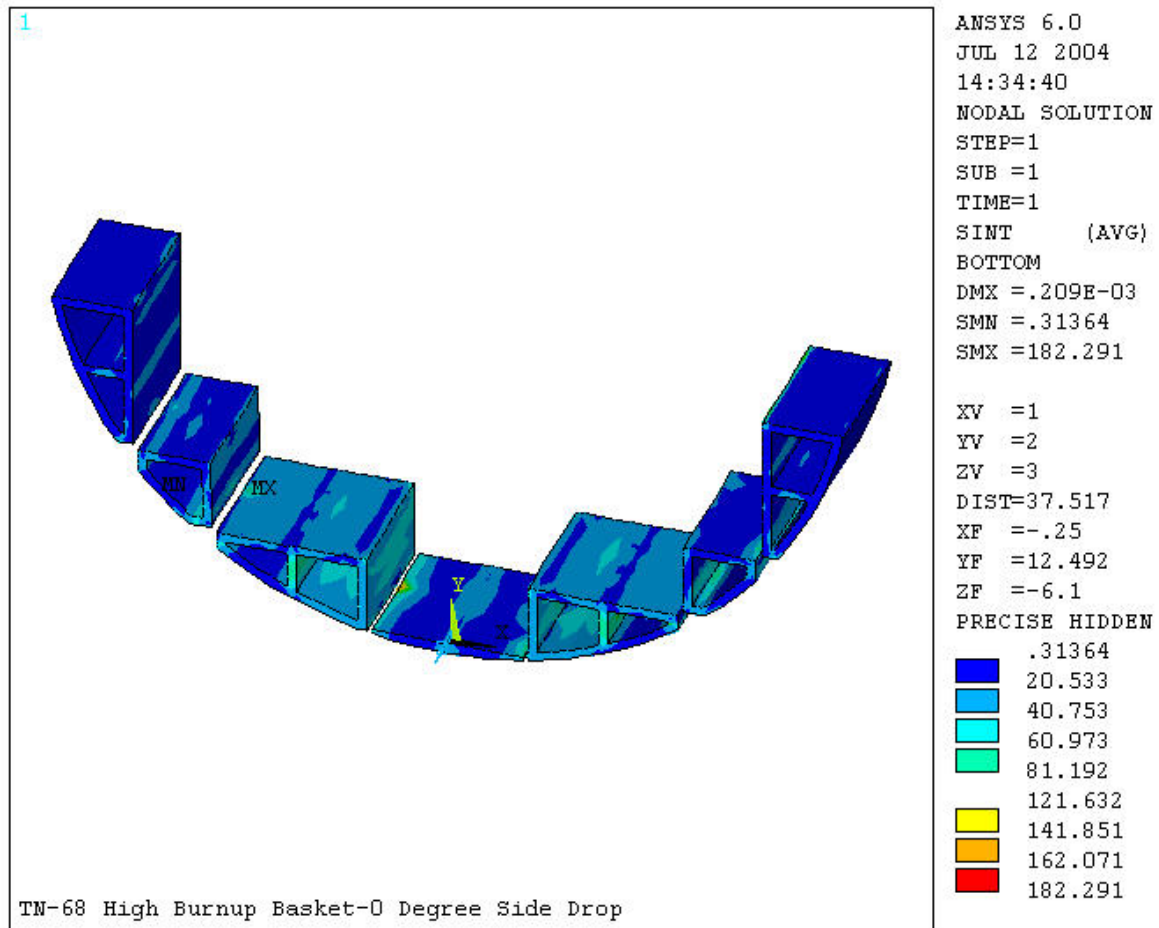


Figure 3B.3-17
Nodal Stress Intensity (Aluminum Rails)-30 Degree Drop

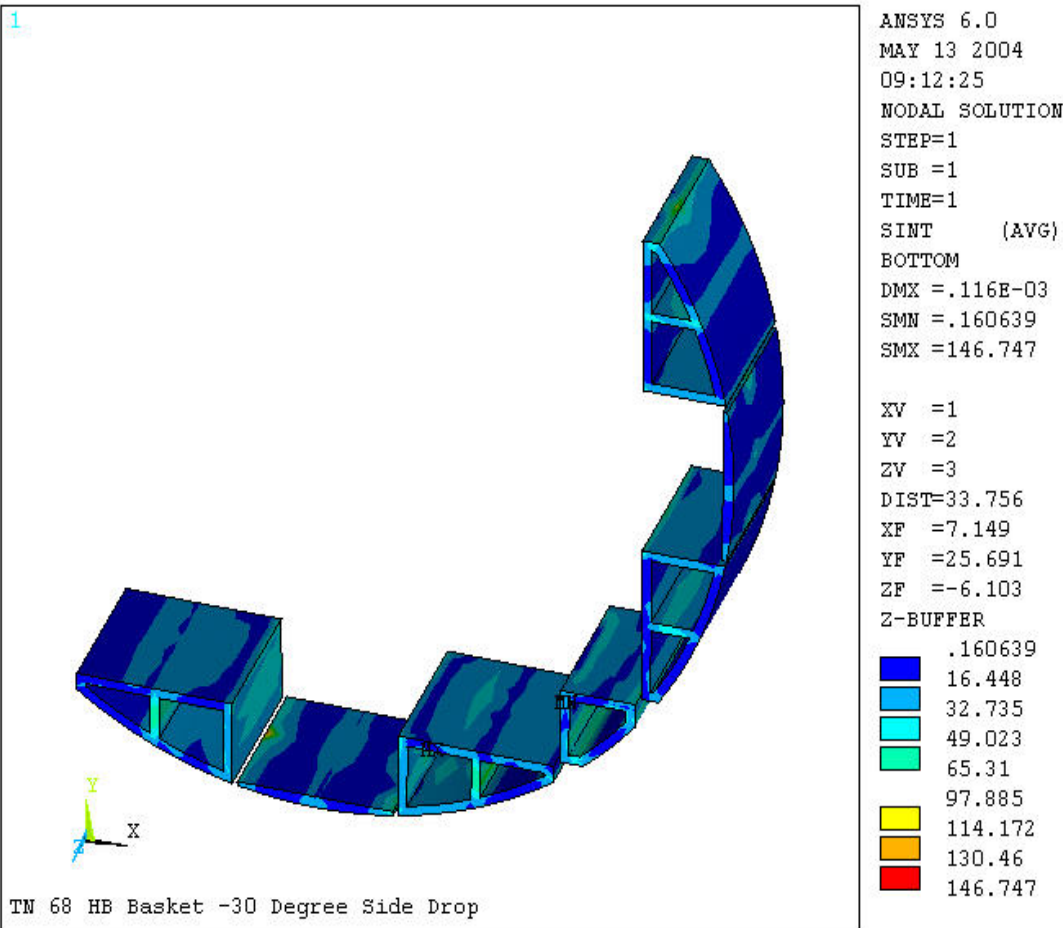
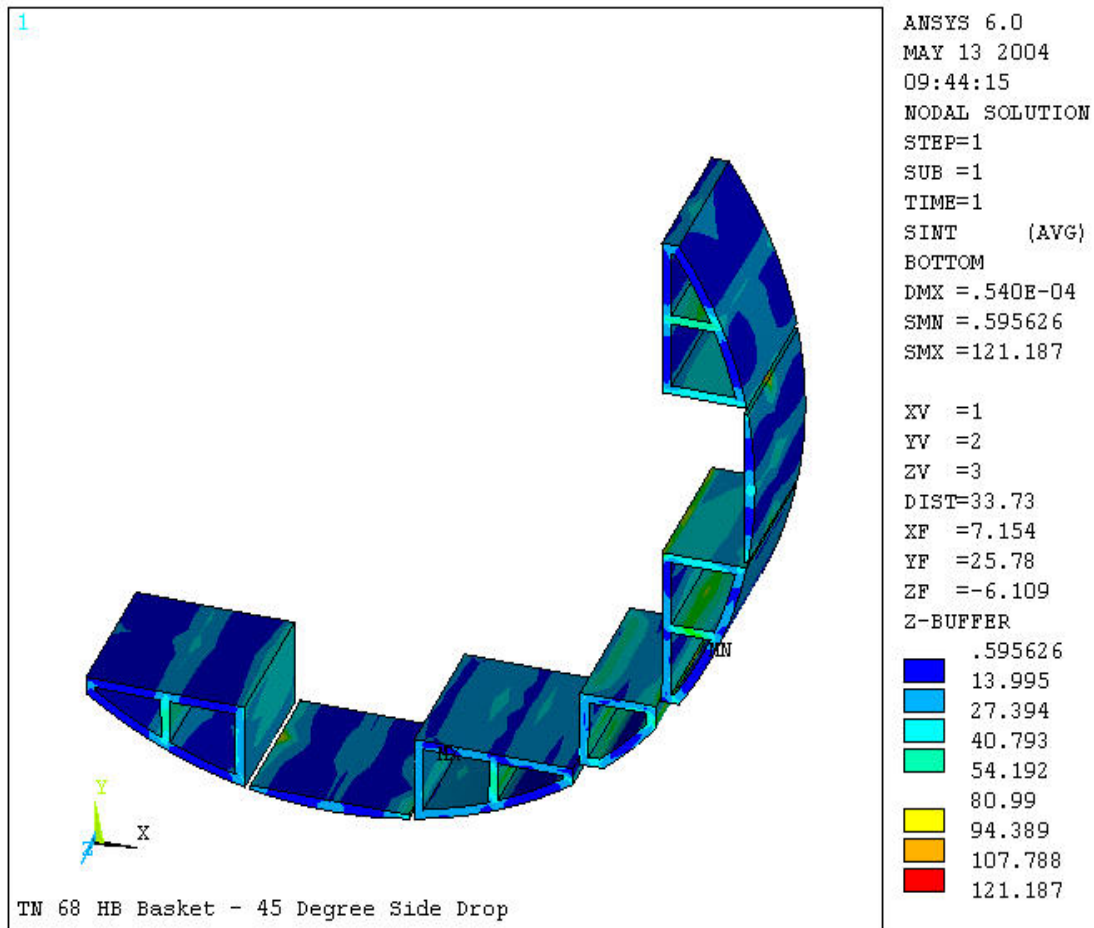
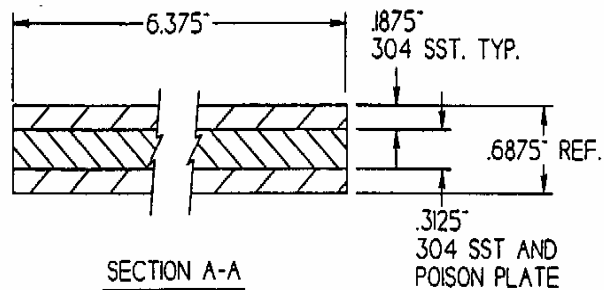


Figure 3B.3-18
Nodal Stress Intensity (Aluminum Rails)-45 Degree Drop





WEIGHT OF 3/16" SST:
 $2 \times 6.375" \times .1875" \times 164" \times .29 = 114 \text{ LBS.}$

WEIGHT OF POISON PLATE:
 $13 \times 6.375" \times .3125" \times 10.4" \times .1 = 27 \text{ LBS.}$

WEIGHT OF 5/16" SST:
 $13 \times 6.375" \times .3125" \times 1.75" \times .29 = 13 \text{ LBS.}$

WEIGHT OF 3/8" SST (BASKET HOLDDOWN):
 $1 \times 6.375" \times .375" \times 13.25" \times .29 = 9 \text{ LBS.}$

TOTAL WEIGHT (IG) = $114 + 27 + 13 + 9 = 163 \text{ LBS.}$

AREA OF 304 SST = $2 \times 6.375" \times .1875" = 2.39 \text{ IN.}^2$

COMPRESSIVE STRESS AT THE BOTTOM OF THE PANEL (3G)

$$\sigma = \frac{3 \times 163}{2.39} = 205 \text{ (PSI)}$$

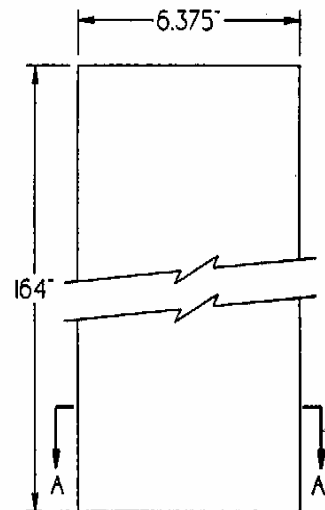
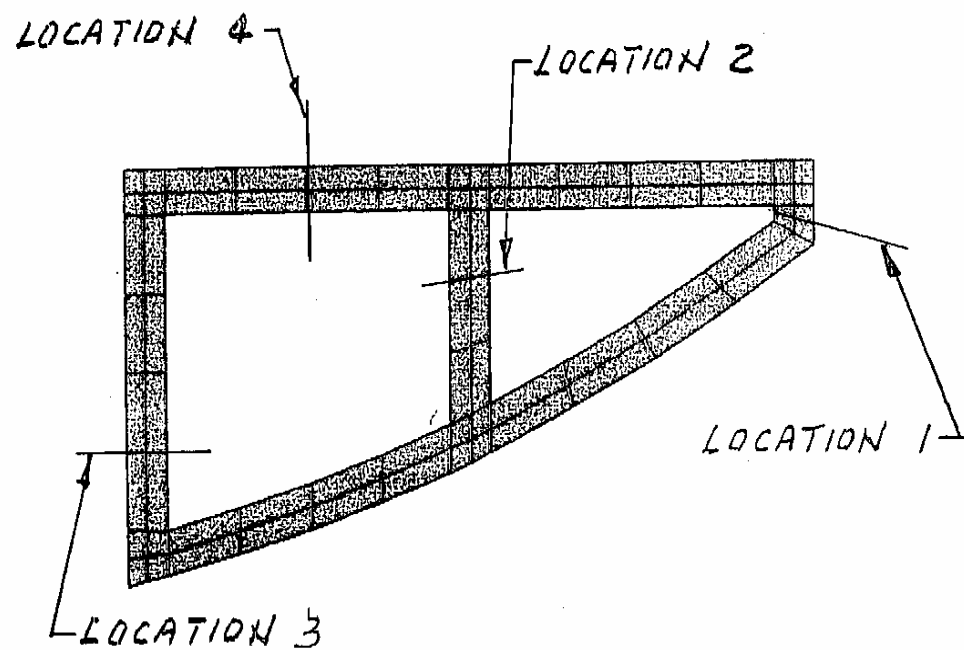


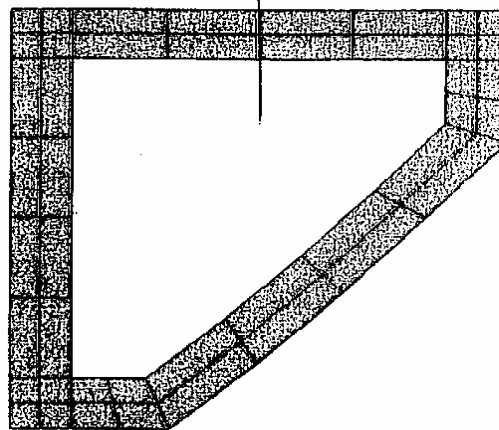
FIGURE 3B.3-19
 BASKET STRESS DUE TO 3G
 VERTICAL LOAD



R-X

FIGURE 3B.3-20
STRESS REPORT LOCATION
(BIG RAIL)

LOCATION 5



x

FIGURE 3B.3-21
STRESS REPORT LOCATION
(SMALL RAIL)

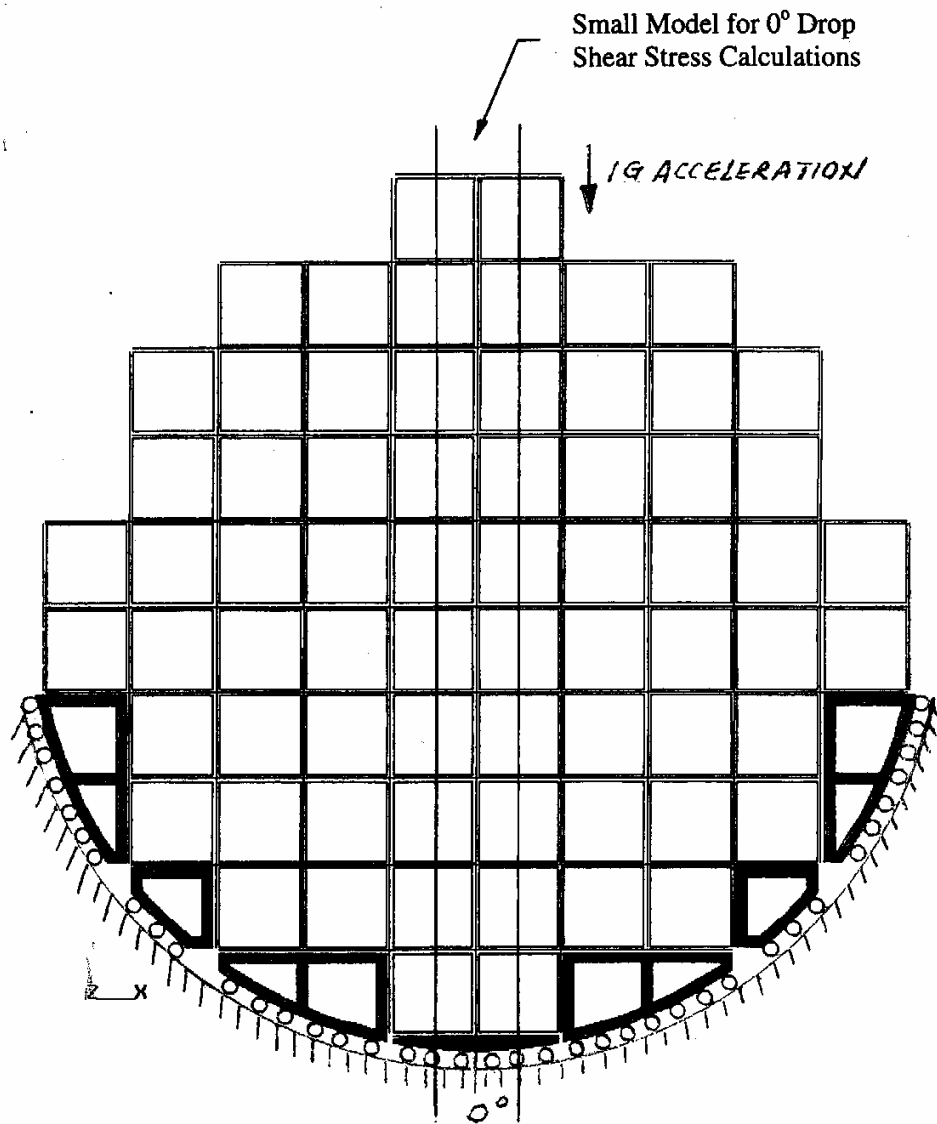


FIGURE 3B.3-22
EXTRACTION OF PARTIAL BASKET MODEL
(FUSION WELDS)

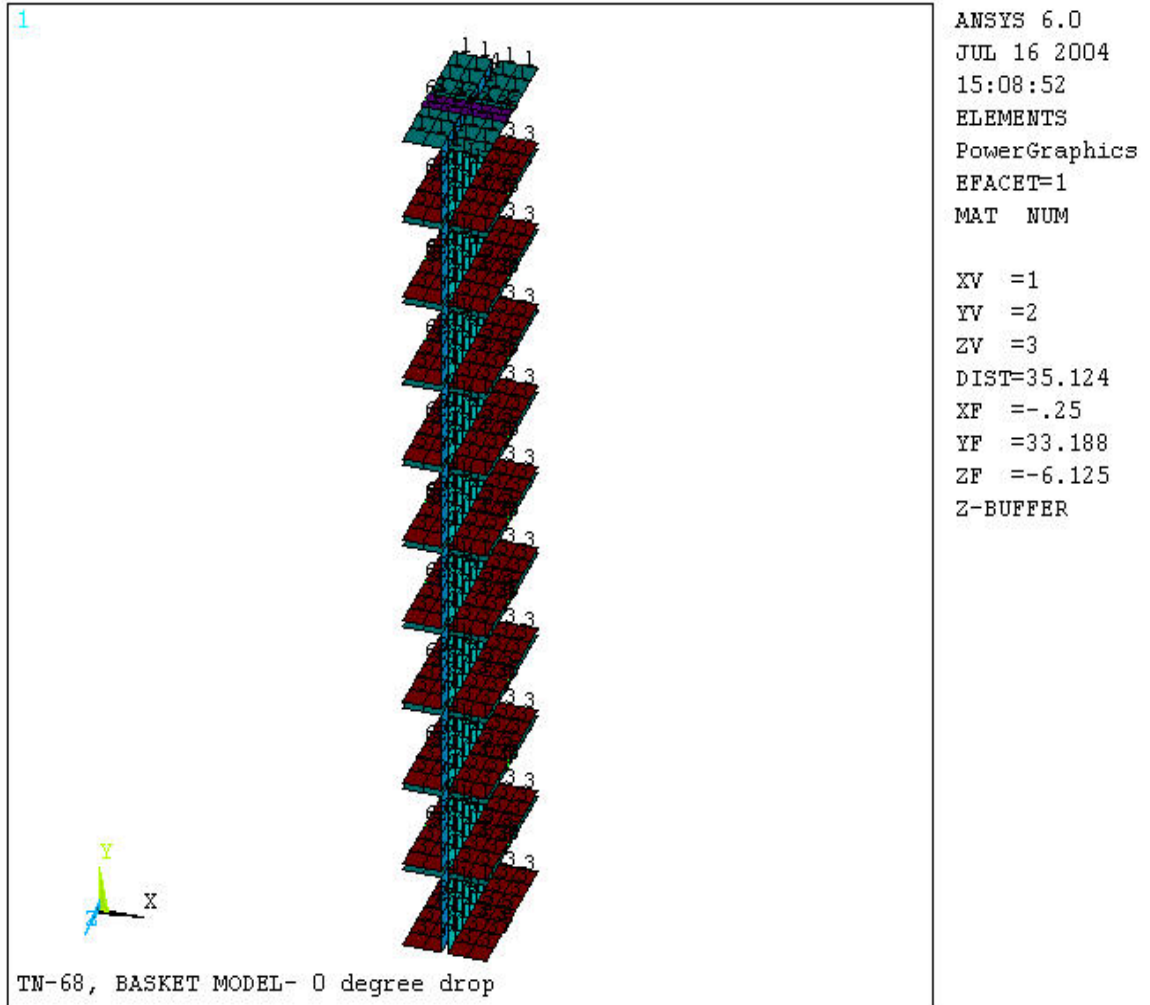


FIGURE 3B.3-23
BASKET PARTIAL MODEL
(FUSION WELDS)

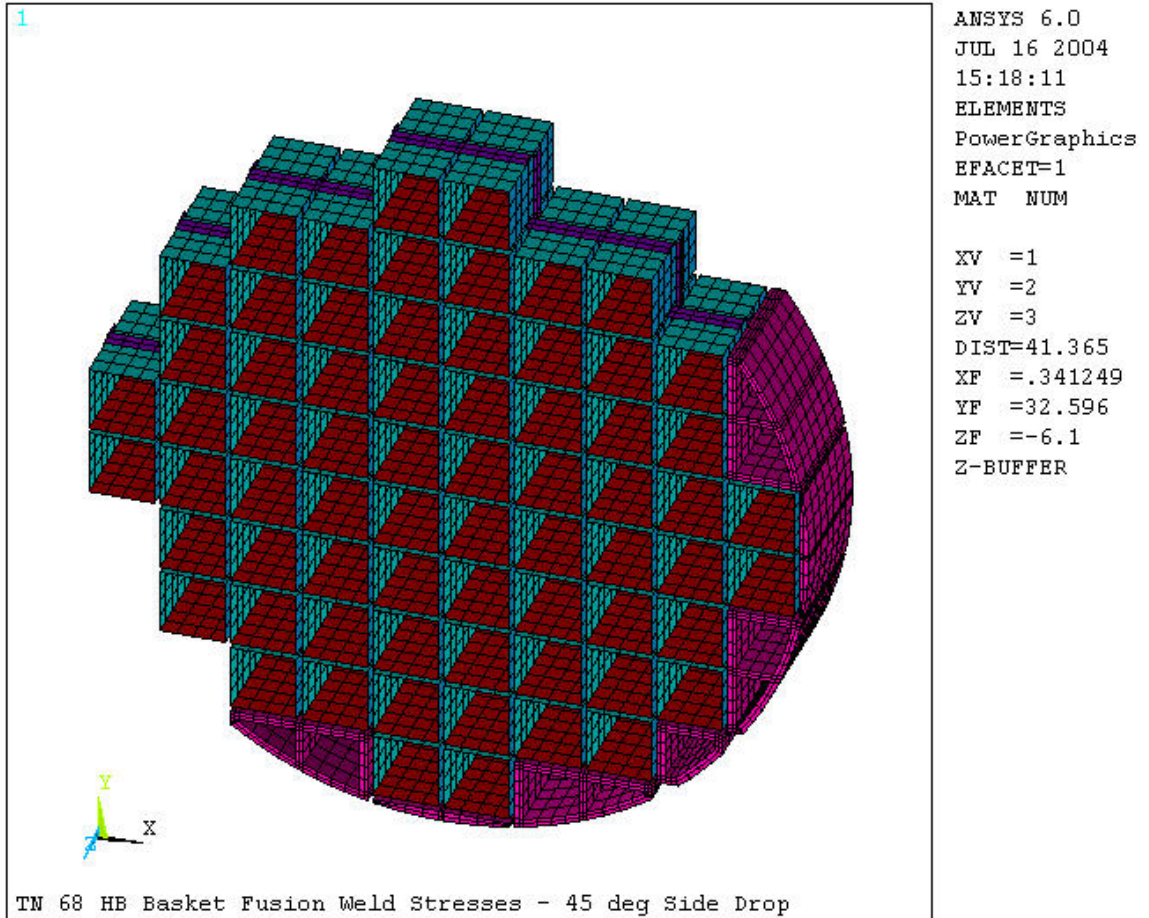


FIGURE 3B.3-24
BASKET FULL MODEL
(FUSION WELDS)

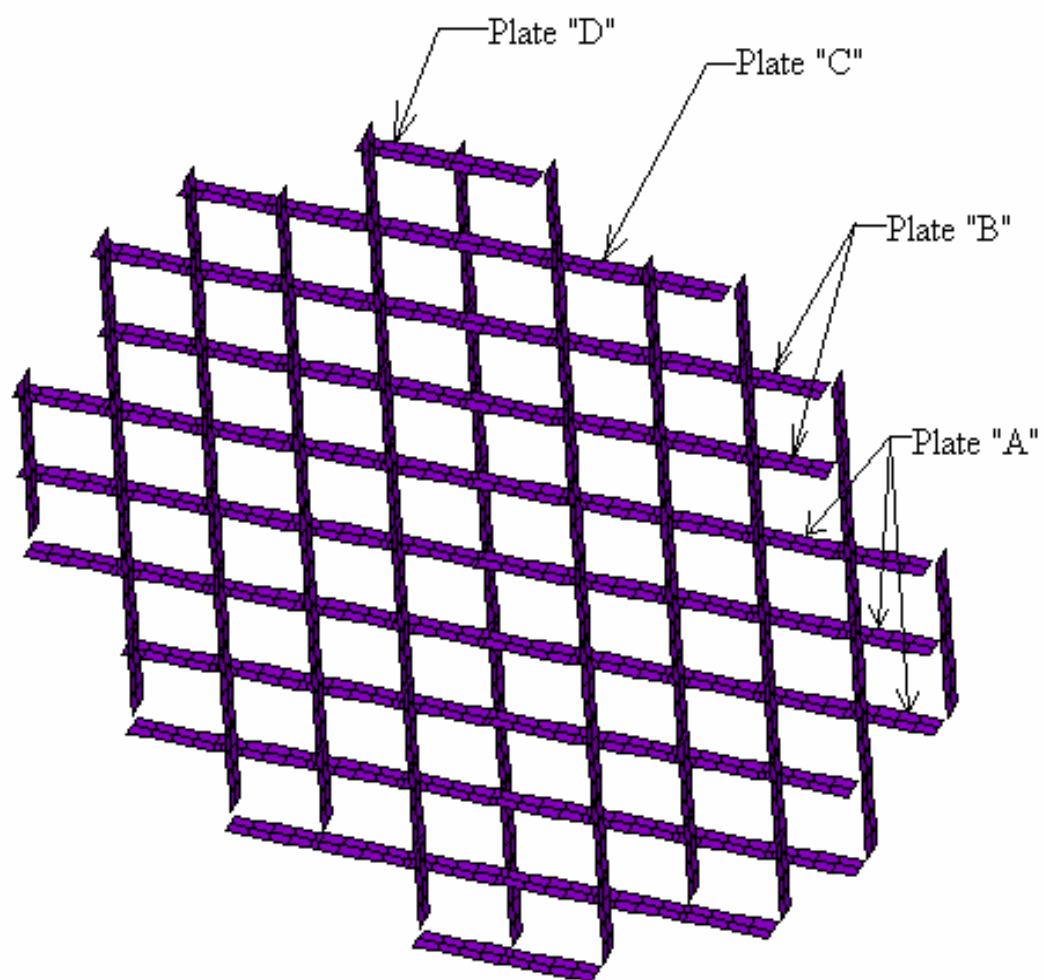


FIGURE 3B.3-25
LOCATION OF BASKET
SUPPORT PLATES

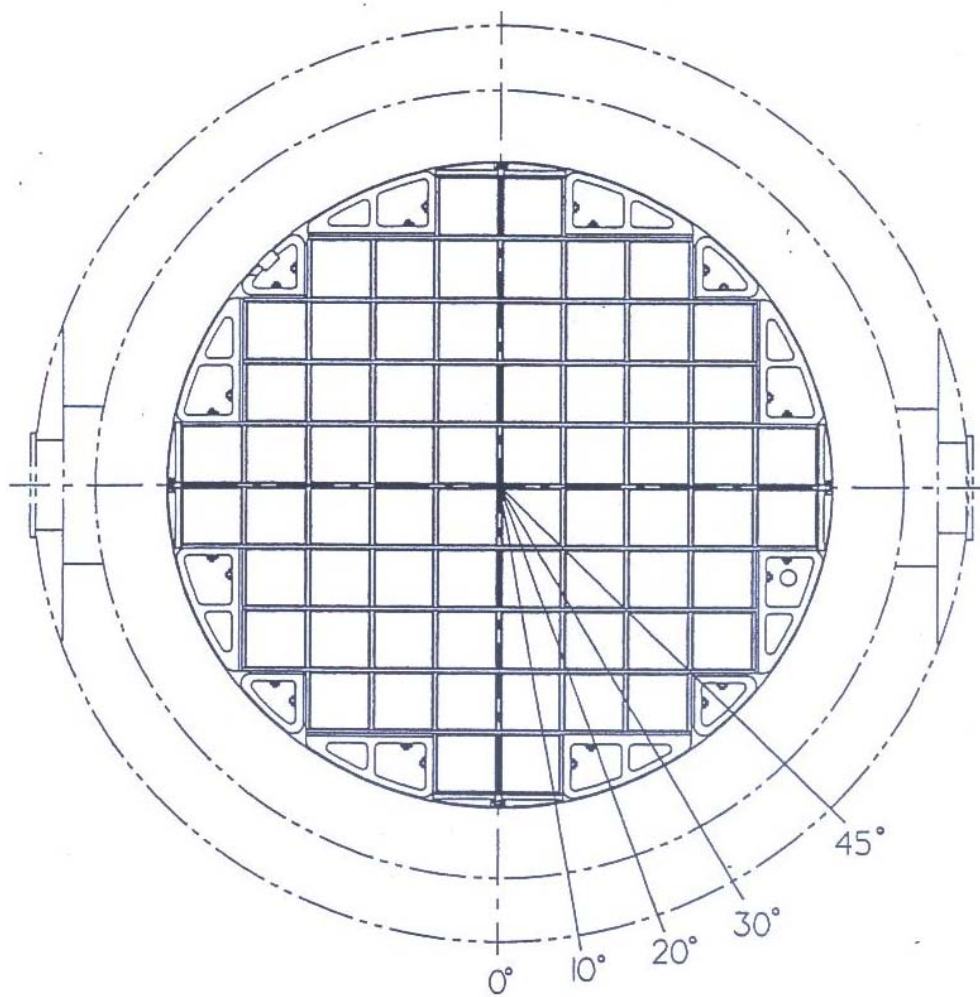
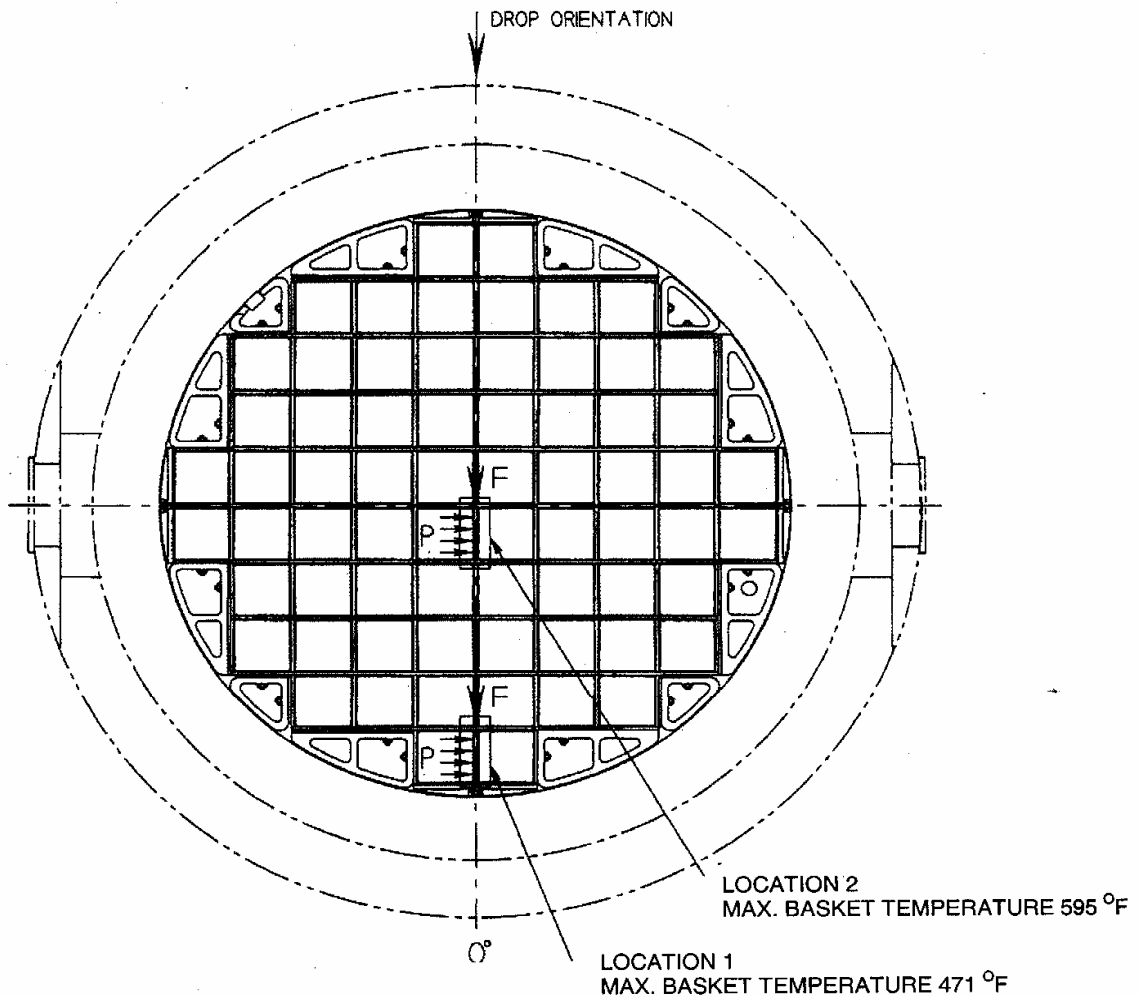


FIGURE 3B.5-1
DROP ORIENTATION



F = TOTAL WEIGHT ABOVE
THE BOTTOM PANEL
(SST AND POISON PLATES,
FUEL ASSEMBLIES, AND RAILS)

P = PRESSURE FROM FUEL ASSEMBLY
DUE TO DROP ORIENTATION
OTHER THAN 0°

FIGURE 3B.5-2
FINITE ELEMENT MODEL
SIMULATION

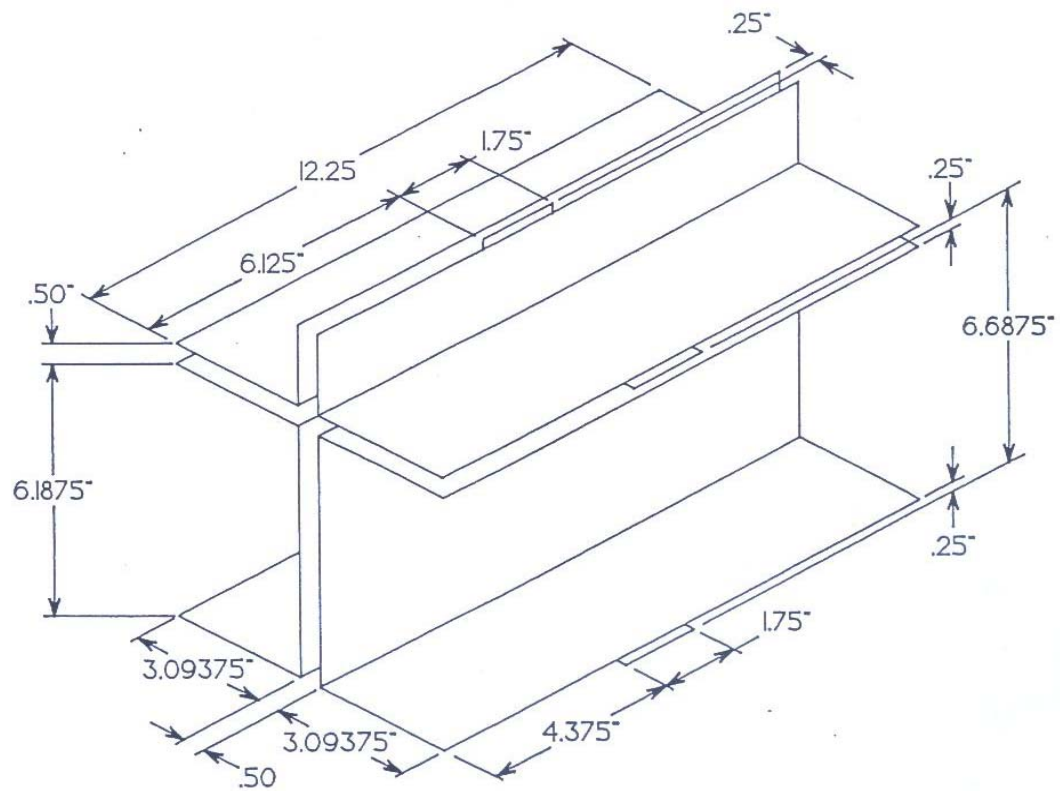


FIGURE 3B.5-3
FINITE ELEMENT MODEL
GEOMETRY

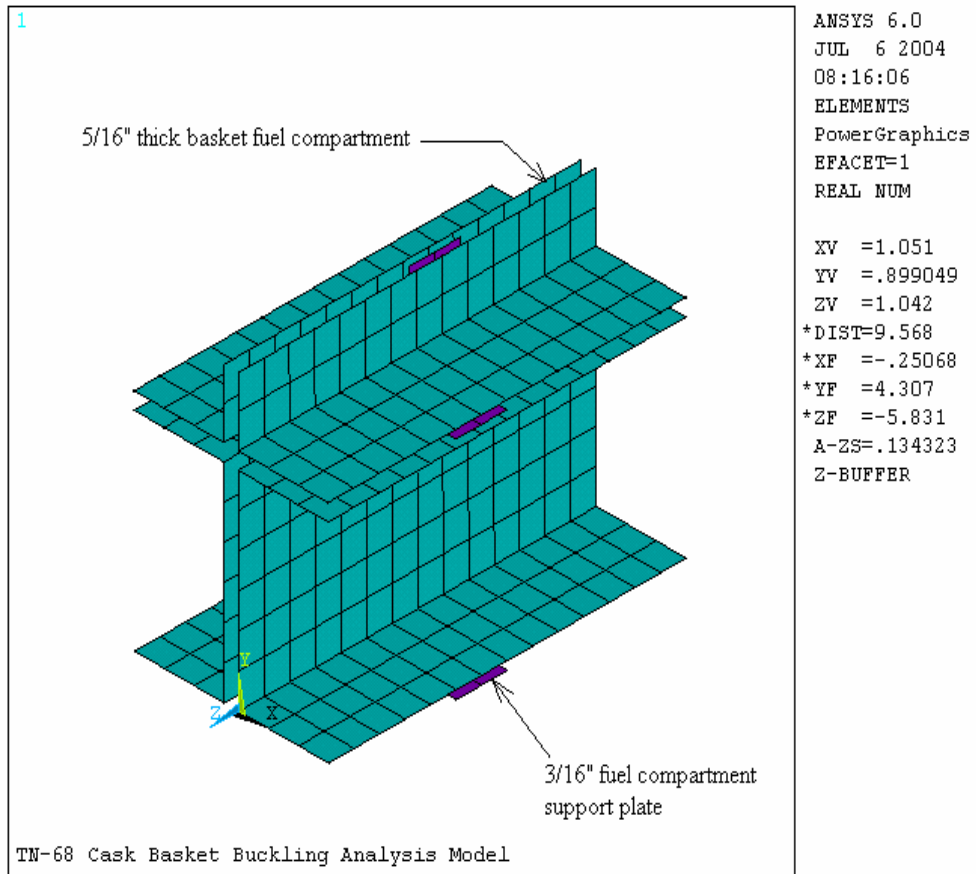


FIGURE 3B.5-4
FINITE ELEMENT MODEL PLOT

F- TOTAL WEIGHT ABOVE
THE BOTTOM PANEL
(SST AND POISON PLATES,
FUEL ASSEMBLIES, AND RAILS)

P- PRESSURE FROM FUEL ASSEMBLY
DUE TO DROP ORIENTATION
OTHER THAN 0°

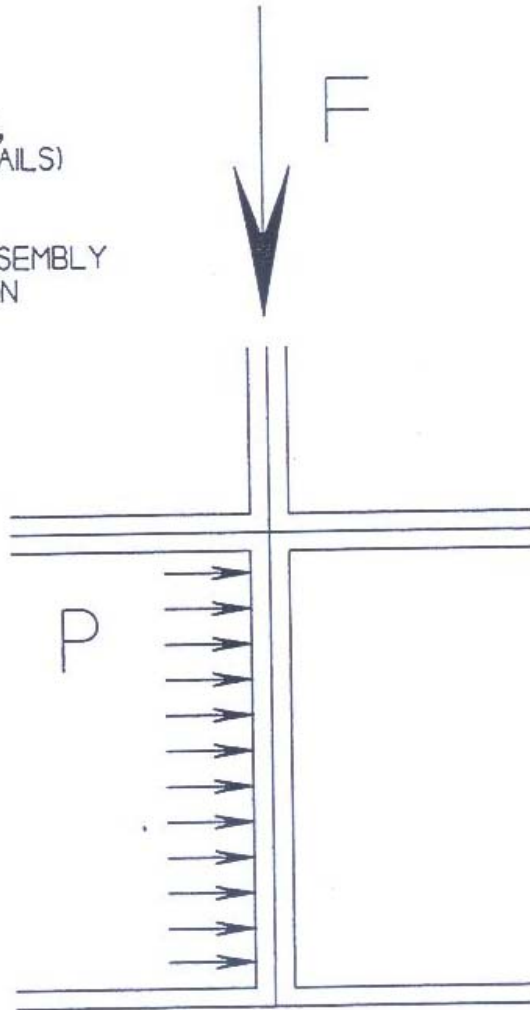


FIGURE 3B.5-5
LOADING CONDITIONS

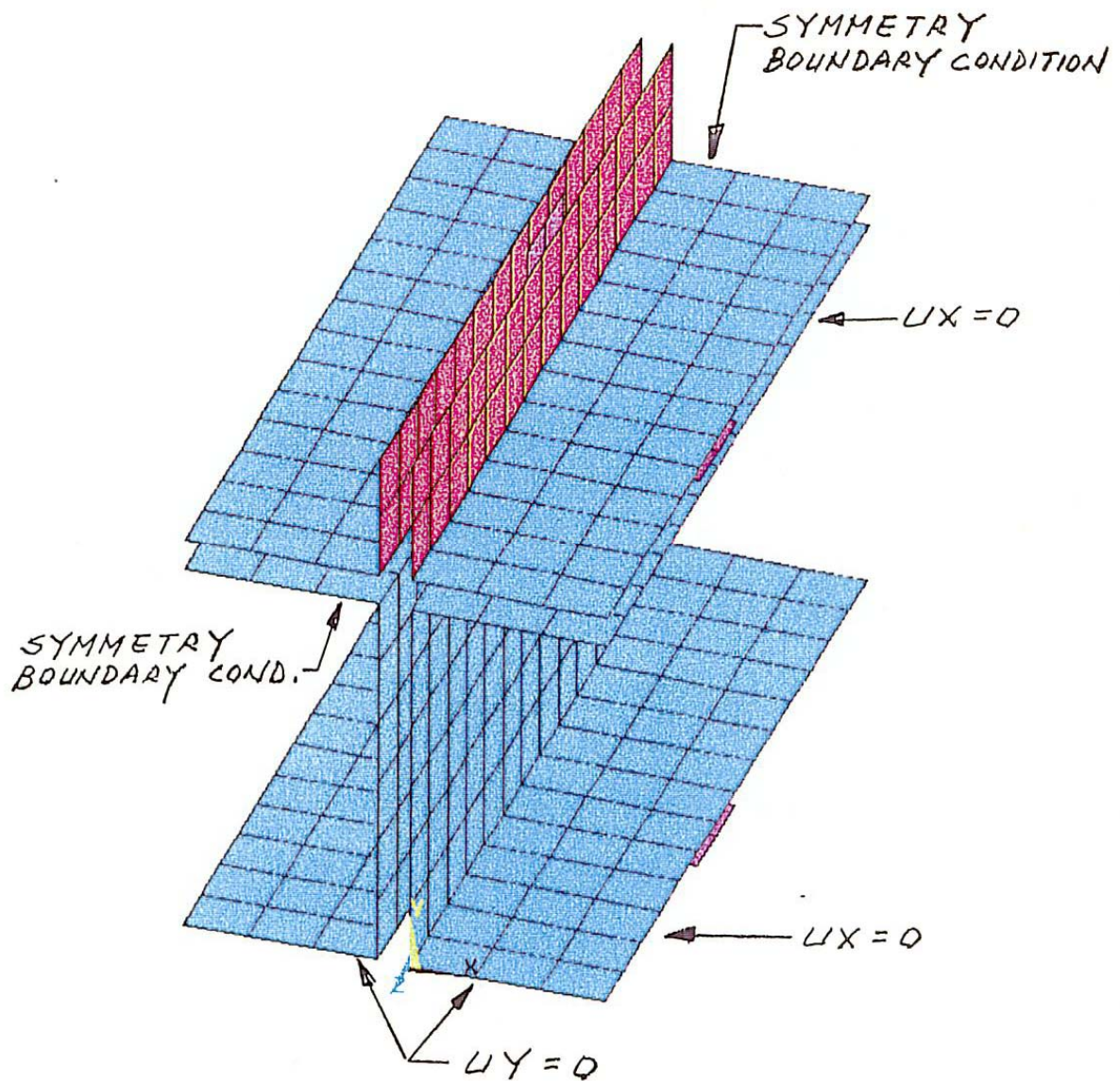


FIGURE 3B.5-6
BOUNDARY CONDITIONS

Figure 3B.5-7
0° Drop Buckling Analysis - ANSYS Computer Plot

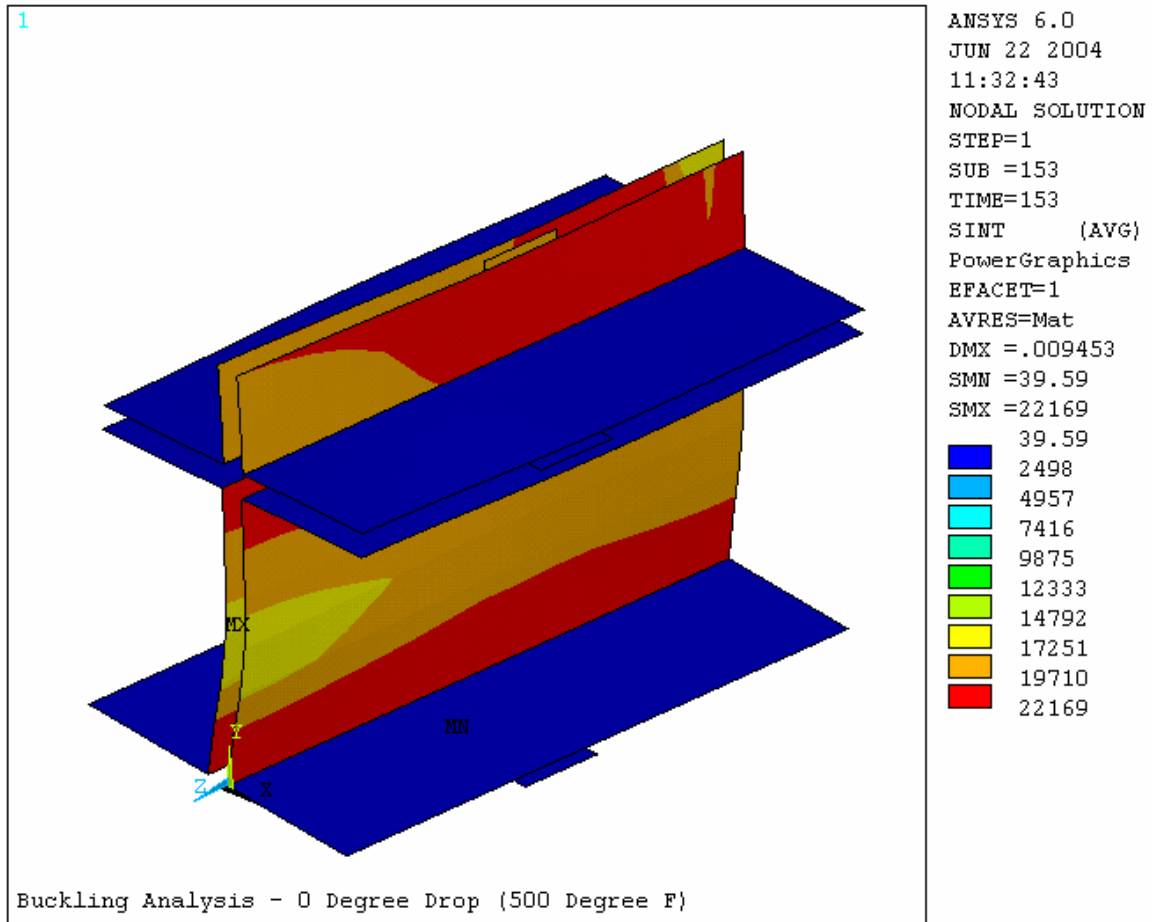


Figure 3B.5-8
10° Drop Buckling Analysis - ANSYS Computer Plot

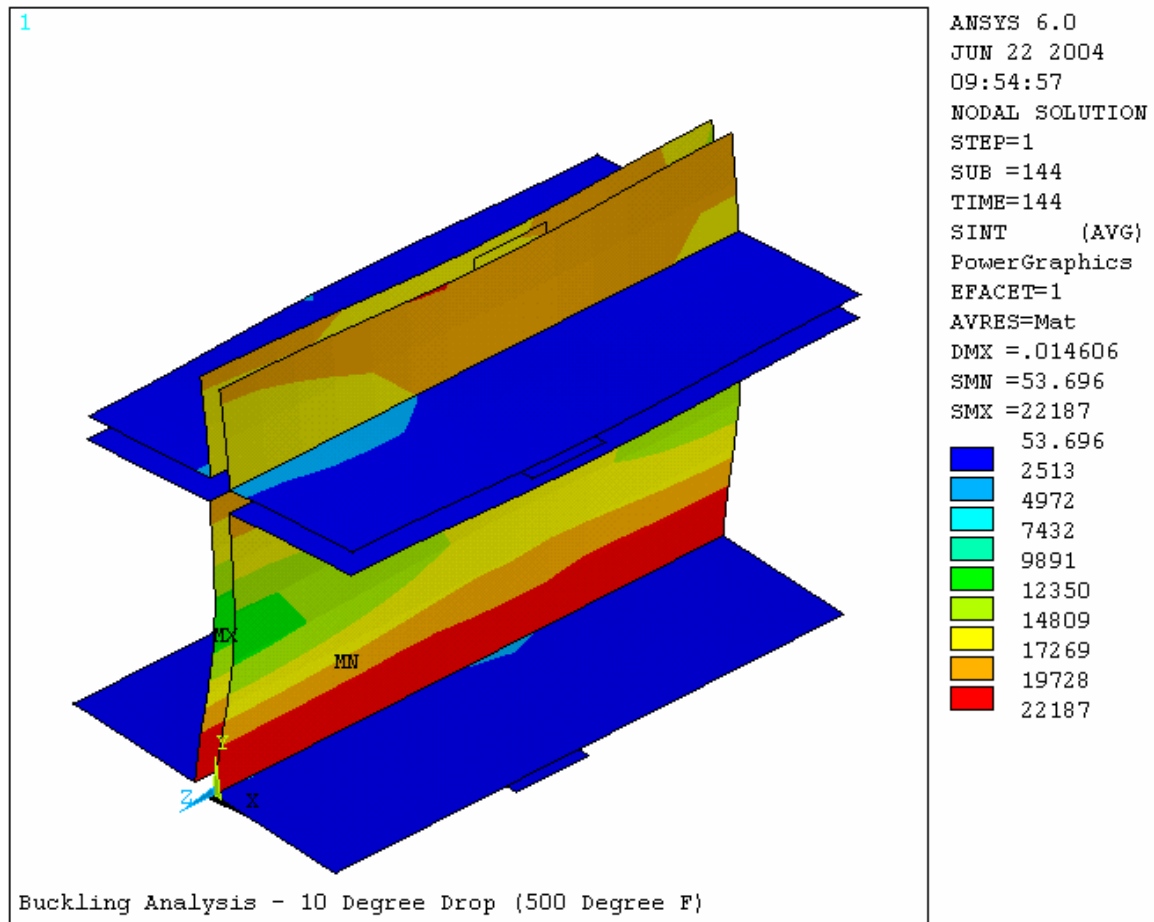


Figure 3B.5-9
20° Drop Buckling Analysis - ANSYS Computer Plot

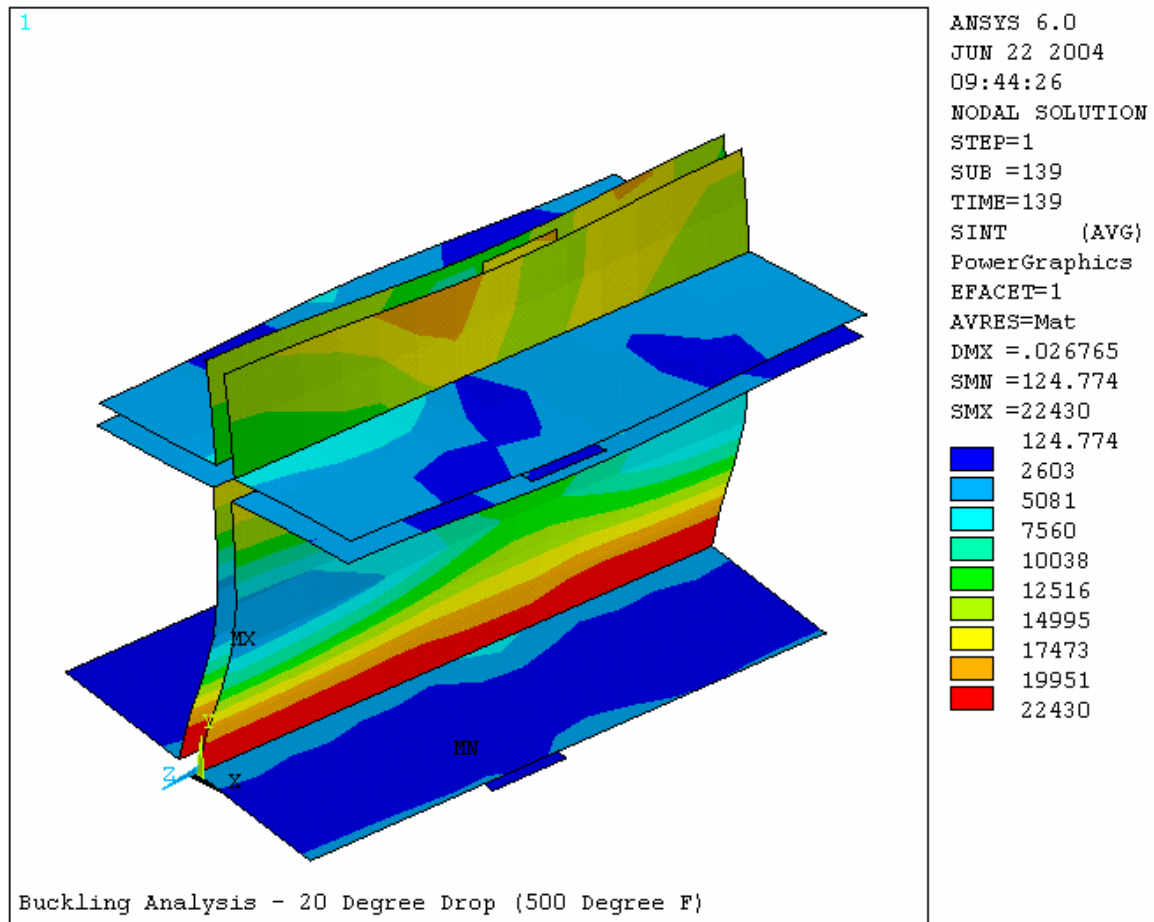


Figure 3B.5-10
30° Drop Buckling Analysis - ANSYS Computer Plot

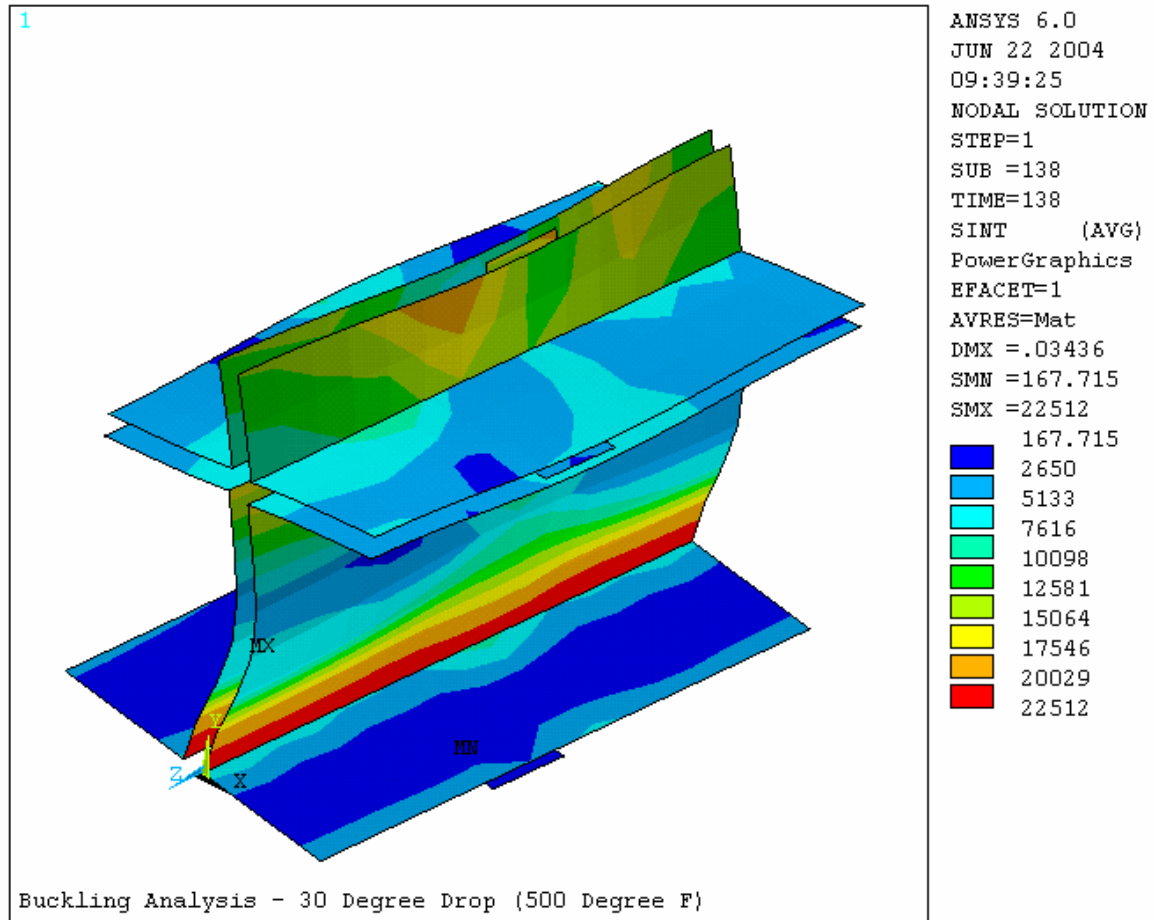


Figure 3B.5-11
45° Drop Buckling Analysis - ANSYS Computer Plot

